Recent advances in biomaterials for 3D scaffolds: A review

Maria P. Nikolova[a,*], Murthy S. Chavali[b,c,d]

[a] Department of Material Science and Technology, University of Ruse "A. Kanchev", 8 Studentska Str., 7000, Ruse, Bulgaria
[b] Shree Velagapudi Ramakrishna Memorial College (PG Studies, Autonomous), Nagaram, 522268, Guntur District, India
[c] PG Department of Chemistry, Dharma Appa Rao College, Nuzvid, 521201, Krishna District, India
[d] MCETRC, Tenali, 522201, Guntur District, Andhra Pradesh, India

ABSTRACT

Considering the advantages and disadvantages of biomaterials used for the production of 3D scaffolds for tissue engineering, new strategies for designing advanced functional biomimetic structures have been reviewed. We offer a comprehensive summary of recent trends in development of single- (metal, ceramics and polymers), composite-type and cell-laden scaffolds that in addition to mechanical support, promote simultaneous tissue growth, and deliver different molecules (growth factors, cytokines, bioactive ions, genes, drugs, antibiotics, etc.) or cells with therapeutic or facilitating regeneration effect. The paper briefly focuses on divers 3D bioprinting constructs and the challenges they face. Based on their application in hard and soft tissue engineering, *in vitro* and *in vivo* effects triggered by the structural and biological functionalized biomaterials are underlined. The authors discuss the future outlook for the development of bioactive scaffolds that could pave the way for their successful imposing in clinical therapy.

1. Introduction

Implantable 3D scaffolds are used for restoration and reconstruction of different anatomical defects of complex organs and functional tissues. The scaffolds provide a template for the reconstruction of defects while promoting cell attachment, proliferation, extracellular matrix generation, restoration of vessels, nerves, muscles, bones, etc. Scaffolds are three-dimensional (3D) porous, fibrous or permeable biomaterials intended to permit transport of body liquids and gases, promote cell interaction, viability and extracellular matrix (ECM) deposition with minimum inflammation and toxicity while bio-degrading at a certain controlled rate. The artificial material substituted for tissue grafts is called alloplastic. The alloplastic bioactive scaffolds ensure not only the mechanical support of the tissue but also serve as a delivery vehicle for bioactive molecules (cytokines, inhibitors, drugs, antibiotics, etc.) and templates for attaching genetically transduced cells establishing new centres for tissue regeneration and morphogenesis. Simultaneously, 3D scaffolds can be used as tissue models replicating the structural complexity of the living tissues. For that reason, not only the biomaterial used, but also the macro-, micro-, and nano-architecture of the scaffolds are of prime importance.

Based on their chemical composition, biomaterials used for 3D scaffolds are classified into metals, ceramics and glass-ceramics, natural and synthetic polymers, and composites. Recently, the focus is put towards biodegradable biomaterials that do not need to be explanted from the organism. Table 1 summarizes the main classes of biomaterials used in 3D scaffold production together with their common application and synthesis methods. Each biomaterial has specific chemical, physical, and mechanical properties, the ability for processing and control of 3D shapes and geometry. The selection of production technique depends on the specific requirements for the scaffold, material of interest, and machine limitation [1]. The integration of computer-aided design (CAD) software and rapid prototyping proposes the ability to produce objects with macro- (overall size and shape), micro- (pore size, shape, interconnection, and distribution) and sometimes nanoarchitecture (nano-roughness, topology, etc.) control of highly complex biomedical devices. Using patient data, the design of the scaffold could be individualized by preparing special 3D model with certain porosity or structures for vasculature that is compatible with multiple biomaterials and cells. The use of 3D printing has revolutionized the development of regenerative medicine and pharmaceutical field.

Recently, much research has been done to develop a variety of novel biomaterials and composites with enhanced cell viability, cell proliferation, and printability. For additional modification, biomimicry approach arranging different cellular components (growth factors, hormones, ECM proteins, etc.) to mimic living tissue is used to enhance

---

Abbreviations

2D	two-dimensional
3D	three-dimensional
3T3	fibroblasts cells
ALP	alkaline phosphatase
ADMSCs	adipose tissue-derived mesenchymal stem cells
BG	bioactive glass
bFGF	basic fibroblast growth factor
BMP-2	bone morphogenic protein-2
BMSCs	bone marrow stromal cells
BSA	bovine serum albumin
CPC	calcium phosphate cement
CSH	calcium sulphate hydrate
CT	computed tomography
dECM	decellularized extracellular matrix
DMSO	dimethyl sulfoxide
DNA	deoxyribonucleic acid
EBM	electron-beam melting
ECM	extracellular matrix
EGF	epidermal growth factor
EPCs	endothelial progenitor cells
FHAp	fluorhydroxyapite
FDM	fused deposition modelling
GF	growth factor
GO	graphene oxide
HA	hyaluronic acid
HAp	hydroxyapatite
hADSCs	human adipose-derived stem cells
hAVICs	human aortic valvular interstitial cells
hBMSCs	human bone marrow-derived stem cells
hDFCs	human dental follicle cells
hEKCs	human embryonic kidney cells
hFOBCs	human fetal osteoblast cells
hNDFs	human neonatal dermal fibroblasts
hTMSCs	human inferior turbinate-tissue derived mesenchymal stromal cells
hUCMSC	human umbilical cord mesenchymal stem cells
hUVECs	human umbilical vein endothelial cells
hUVSMCs	human umbilical vein smooth muscle cells
LBM	laser beam melting
MBG	mesoporous bioactive glass
MC3T3-E1	osteoblast precursor cell line
MG-63	human osteosarcoma cell line
MRI	magnetic resonance imaging
MSC	mesenchymal stem cells
MWCNTs	multi-wall carbon nanotubes
NHEKs	normal human epidermal keratinocytes
oMSCs	ovine mesenchymal stem cell
PAA	poly(acrylic acid)
PCL	ε-poly(caprolactone)
PEG	poly(ethylene glycol)
PEI	polyethyleneimine
PEO	poly(ethylene oxide)
PES	polyethersulphone
PET	polyethylene terephthalate
PGA	poly(glycolic acid)
PGF	platelet-derived growth factor
PHB	polyhydroxybutyrate
PHBV	poly(3-hydroxybutyrate-*co*-3-hydroxyvalerate)
PHEMA	polyhydroxy ethyl methacrylate
PHPMA	N-(2-Hydroxypropyl)methacrylamide
PLC	poly(ʟ-lactide-*co*-ε-caprolactone)
PLGA	poly(lactic-*co*-glycolic) acid
PLA	poly(lactic acid)
PLLA	poly(ʟ-lactic acid)
P(LLA-CL)	poly(ʟ-lactic acid-*co*–caprolactone)
PMMA	poly(methyl methacrylate)
PP	polypropylene
PU	polyurethane
PVA	polyvinyl alcohol
PVAc	polyvinyl acetate
rBMSC	rat bone mesenchymal stem cells
rCCs	rabbit corneal cells
rGO	reduced graphene oxide
rhBMP-2	recombinant human bone morphogenic protein-2
RNA	ribonucleic acid
SDSCs	synovium-derived stem cells
SH-SY5Y	human-derived cells used as models for neuronal function and differentiation
SiHAp	silicate containing hydroxyapatite
SLA	stereolithography
SLS	selective laser sintering
TGF-β1	transforming growth factor-β1
TPU	thermoplastic polyurethane
VEGF	vascular endothelial growth factor
β-TCP	β-tricalcium phosphate

cell signalling or ECM formation [2]. Moreover, biomaterial scaffolds are used for delivering therapeutic agents like proteins, growth factors, drugs, etc. and the anchorage of these substances to the scaffold is of high importance for loading. As biomaterial-cell interactions are key to cell viability, proliferation and differentiation, characteristics of biomaterials such as surface chemistry, charge, roughness, reactivity, hydrophilicity, and rigidity need to be considered. With continuous research and progress in biomaterials used in medical implants, the goal of this review is to discuss recently developed implantable scaffold materials for different tissues and highlight the advances in *in vitro* and *in vivo* biological regeneration.

2. 3D scaffold requirements

A large number of scaffolds with various macro- and micro-architectures from different biomaterials have been reported in the literature. The design of a scaffold includes mechanical (stiffness, elastic modulus, etc.), physicochemical (surface chemistry, porosity, biodegradation, etc.), and biological (cell adhesion, vascularization,

biocompatibility, etc.) requirements as well as considerations concerning sterilization and commercial feasibility. To improve the bioactivity and functionality of 3D scaffolds acting as synthetic frameworks or matrices, the shape, size, strength, porosity, and degradation rate are readily controlled. The design of these regeneration templates has evolved over the past years. To repair the damaged tissue, the scaffold should be designed and fabricated in a manner resembling the anatomical structure and mimicking the function and biomechanics of the original tissue. The 3D scaffold should temporarily withstand the external loads and stresses caused by the formation of the new tissue while preserving mechanical properties close to that of the surrounding tissue. It was demonstrated that the tissue-specific mechanical characteristics, in particular, stiffness, could control the differentiation of MSCs [3]. Simultaneously, the scaffold designs such as sponges, meshes, foams, etc., are able the control biodegradation as a key factor in tissue engineering. The degradation of biomaterials could be surface or bulk. In contrast to bulk degradation that breaks the internal structure of the material, the surface degradation maintains the bulk structure. The rate of degradation should match the tissue growth without

Table 1
Biomaterials for 3D scaffolds production together with their common application and fabrication methods.

	Class biomaterial			Application	Fabrication
Biomaterial for 3D scaffolds	CERAMICS		(*HA, β-TCP, α-TCP, ZrO₂, TiO₂, porous bioglass, calcium silicate, calcium sulphate, etc.*)	Hard tissue replacement Orthodontic application	- Binder jetting/inkjet printing - Extrusion - Stereolithography - SLS - Laser aid gelling - FDM - Polymer sponge replica - Salt leaching - Dual-phase leaching - Gel casting
	POLYMERS	Natural	**Proteins** (*silk, collagen, gelatin, fibrinogen, actin, keratin*) **Polysaccharides** (*alginate, chitosan, cellulose, dextran, chitin, glycosaminoglycan, hyaluronic acid, agarose*) **Polynucleotides** (*DNA, RNA*)	Connective and hard tissue application Decellularized living tissues/organs Drug delivery Hard and soft tissue on applicants Gene therapy	- Solvent casting - Inkjet printing - Particle aggregation - Micro moulding - Photolithography - Emulsification - Electrospinning - Cryo-gelation - Sol-gel
		Synthetic	**Degradable** (*polyesters, polyorthoesters, polylactones, polycarbonates, polyanhydrides, polyphosphazenes, etc.*) **Non-degradable** (*PE, PTFE, PMA, PAA, PU, polyether, polysiloxanes, etc.*)	Drug-delivery systems Implants Orthopaedic implants	- SLA - SLS/SLM - EBM - FDM - Polyjet - Electrospinning - Phase separation - Freeze drying - Gas foaming - Inverse opal hydrogelation - Self-assembly
	METALS & ALLOYS		(*Co–Cr, Ti, Ti–6Al–4V, stainless steel etc.*)	Orthopaedic and dental application Artificial hearing	- SLA - SLM - SLS - EBM - Powder metallurgy - Vacuum foaming - Directional solidification
	COMPOSITES		Blends of polymers and ceramics/metals	Orthopaedic and dental application	- Textile base fabrication - Laminated object manufacturing (LOM) - FDM - SLA - Freeze-drying method

separation of toxic byproducts. The degradation of a biomaterial could be achieved by physical, chemical, biological or combined processes influencing the biocompatibility of the 3D scaffold. For example, incorporating different biodegradable components in the construct triggers hydrolytic degradation while processes such as enzymatic digestion and cell-driven degradation biologically change the implant material. When the application of a scaffold does not require a complete degradation (for example in articular cartilage repair) permanent (non-degradable) or semi-permanent scaffolds could be used. When implanted in body right, toxic, immunological or foreign body responses should not occur which prove the scaffold biocompatible. The surface properties of a scaffold should also be designed in such a way that to facilitate cell attachment, homogeneous distribution, proliferation and cell-to-cell contacts. The scaffold geometry should maintain the porous or fibrous design and provide high surface-to-volume ratio for cell attachment and tissue development. Nanostructured surfaces demonstrate high surface energy as opposed to polished materials that result in enhanced hydrophilicity and, therefore, improved adhesion of proteins and cell attachment. For metal and ceramic scaffolds, the smaller grain size not only increases the mechanical strength but was found to be more favourable in terms of attachment and proliferation of osteogenic cells [4]. Therefore, the scaffold with its topography and mechanical features controls cellular behaviour. When seeded in 3D scaffolds, cells need to be urged to regain typical *in vivo* morphology.

The process of regeneration also requires the development of interconnected neurovascular networks between the mature and surrounding tissue. On one hand, the scaffold design should make allowance for vascular remodelling as tissue mature so that nutrients, oxygen and other soluble factors could reach all embedded cells while the metabolic wastes are constantly removed. On the other hand, nerve fibres are spatially closely associated with cells that express receptors for neuropeptides and should be simultaneously developed with the new tissue to regulate homeostasis. Usually, the distribution of peripheral nerves and blood vessels follows each other in human body development because they are anatomically coupled and influence the growth and development of each other [5]. Since it is still hard to regulate multi-tissue types development, autologous neurovascular bundles integrated by microsurgery during scaffold implantation is a potential concept [6] for improving scaffold performance.

To support and accelerate the endogenous healing process, especially in extensive or irreversible damages, different strategies for administration of stem cells (after *in vitro* expanded) alone or in combinations with natural or synthetic scaffolds are proposed. Stem cells from different sources (bone marrow, adipose, muscle tissue, lung, umbilical cord, etc.) are usually used as therapeutic rely on because of their ability to maintain homeostasis in healthy tissues and differentiate when activated under a reparative response or disease. When using tissue-specific stem cells, they are able to regenerate the tissue from

which they are isolated. After the injury, a cascade of biological events such as stem cell migration, chemokine and growth factor secretion occurs to repair the destroyed tissue. These processes could be mimicked, stimulated and controlled by adding a variety of bioactive moieties such as growth factors, peptides, genes, aptamers (single strength oligonucleotides), antibodies, drugs, or even ECM. These substances are chemically or physically (by electrostatic forces, hydrophobic interactions, and hydrogen bonds) decorated to the scaffold. In that way, the engineered complex scaffolds mimic natural signalling and repair events and generate suitable microenvironment for adhesion, proliferation, differentiation of stem cells that regenerate the tissue.

3. Types of 3D scaffolds based on their geometry

Scaffolds of various biomaterials cover a wide range of applications (Fig. 1). The classification of these complex constructs could be based on their geometry or material source.

When the geometry is used to categorize 3D scaffolds, the available biological constructs are:

3.1. Porous scaffolds

Sponge or foam porous scaffolds usually contain interconnected pore structure (orientated or random) that is highly useful in bone regrowth, vascularization and ECM deposition. Because of the high physical surface, such scaffolds provide improved gas and nutrients transport through the channel network. However, increased pore interconnectivity is required for peripheral nerve and blood vessels growth without scarifying the mechanical properties of the scaffold. Otherwise, the cell in-growth and flow of nutrients will be prevented. If the pores are too small, the cellular penetration, ECM deposition, and neovascularization could be prevented. Ideally, the interconnected porous structure should consist of 90% porosity [7] which could substantially influence the resulting mechanical properties. However, the ideal size of pores for specific cells and tissues varies substantially [8]. For example, pores with 200–400 μm size were found to be effective for bone tissue formation [9], while 50–200 μm pores were suitable for smooth muscle cell growth [10]. Scaffolds with pore sizes between 10-44 and 44–75 μm enable accommodation only of fibrous tissue [11]. As a rule, pores with sizes greater than 100 μm enable tissue growth and vascularization, whereas micro- (less than 2 nm) and mesopores (2–50 nm) promote cell adhesion and resorbability at controllable rates [12]. The pores that are excessively large in size (more than 400 μm) decrease the cell-to-cell contact ratio since the cells experience two-dimensional (2D) growth pattern on the substrate rather than a 3D organization [6]. The special properties of porous scaffolds could be obtained by using methods capable of applying control over pore sizes. Except for the conventional freeze-drying and solvent casting/particulate leaching techniques, fabrication methods with enhanced control over the porosity are the inverse opal hydrogelation which uses colloidal particles as templates for obtaining ordered macroporous scaffolds or cryogelation utilizing frozen solvent crystals as interconnecting porogen [13].

3.2. Fibrous scaffolds

Fibrous scaffolds from different biodegradable polymers such as PCL [14], PLA [15], PLGA [16], gelatin [17], cellulose [18], silk fibroin [19] have been successfully prepared. Fibres possess the desired properties as scaffolds for skin, cartilage, ligament, bone, muscle, vein and vehicles for drugs, DNA and proteins [20]. Nanofibres as scaffolds are found to be more favourable biomaterials than micro fires because the nanosize provokes cell to obtain typical *in vivo* morphology. Nanofibres have the potential to provide guiding alignment for neurite growth by establishing topographical clues affecting cell differentiation and fate

[21]. These nanofibres mimic the structure and properties of the extracellular matrix and because of their high aspect ratio, porosity, and surface-to-volume ratio, they induce greater cellular attachment than microfibres [22]. The nanostructure may help the rapid diffusion of encapsulated substances and cell infiltration [23]. When cultured on smaller fibres (283 nm) of polyethersulphone (PES) with laminin (protein of ECM, a major component of the basal lamina), rat neural stem cells showed 40% increase in oligodendrocyte differentiation and 20% increase on larger fibres (749 nm) [24]. Commonly used techniques for fabrication of nanofibres are electrospinning, self-assembly, phase separation, and solid free-form fabrication. In electrospinning, by applying electrical field, the ejected material from the syringe pumps forms fibres from nanometers to several micrometres in size producing fibrous scaffolds. During electrospinning high voltage is imposed between the spinneret and the ground collector to thinner the filaments. In order to have stable fibres, polymers with enhanced chain entanglement such as PCL, PLLA, PLGA, and polymer-containing composites, are used. The method has high loading and encapsulation capacity of small molecules and drugs [25]. Phase separation technique separates phases through cooling or non-solvent exchange of heterogeneous fibre structures with little control over diameter and orientation of fibres whereas the self-assembly process autonomously organizes components into nanofibre structures. The phase separation method suffers from drawbacks such as limited material selection and inadequate resolution while self-assembly requires careful molecular design because of the complex mechanism of synthesis. Recently, Yao et al. proposed the production of scaffolds using thermally-induced self-agglomeration of short individual electrospun nanofibres and tiny nanofibre pieces in ethanol/water/gelatin (4/2/1) solution followed by freeze-drying [26]. The hierarchical structure consisted of random overlaid PLC/PLA fibres with a diameter ranging from 150 nm to 2 μm, pores from sub-micron to around 300 μm, and about 96% porosity. It was also found that the aligned fibres are able to direct the tissue growth [27] while random fibres demonstrate improved stiffness in all directions [28]. Yin et al. discovered that aligned PLLA scaffolds induced endogenic differentiation in MSCs while the cells cultured on randomly orientated fibres displayed enhanced osteogenic differentiation [29]. These facts provide inside into development of fibrous scaffold design with smart functionalization in interfacial tissue engineering. For that reason Cai et al. developed dual-layer aligned random nanofibrous scaffolds of electrospun silk fibroin-P (LLA-CL) that effectively augmented tendon-to-bone integration and improved
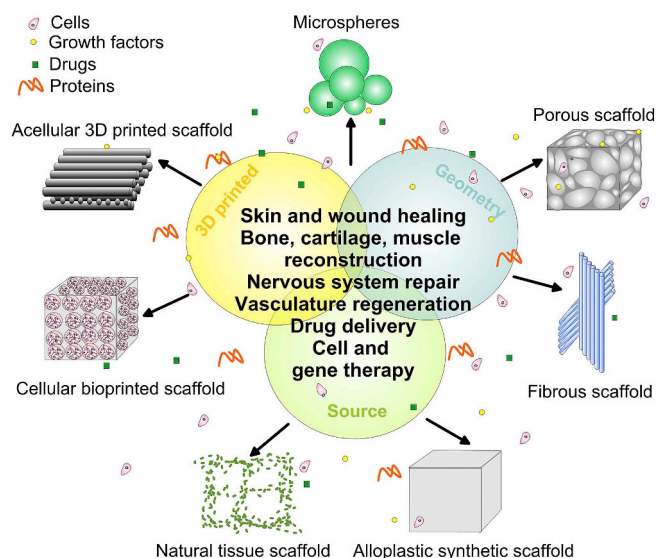

Fig. 1. A general scheme of various types of 3D scaffolds together with their applications in tissue engineering.

gradient microstructure formation [30]. However, the lack of specific functional groups in synthetic nanofibres requires functionalization by attaching different ligands (such as molecules, proteins, ceramics, etc.). Mixed fibre mesh scaffolds provide the opportunity to develop constructs with enhanced properties (biomechanical, physicochemical and biological) in comparison to the properties of individual scaffolds. For example, when nanofibre-reinforced composites are used, higher mechanical strength than traditional unfilled composites could be obtained [31]. Nonetheless, conventional fibre scaffolds suffer from some disadvantages like limited thickness and small pore size.

3.3. Microsphere/microparticle scaffolds

These scaffolds are intensively used in advanced applications such as gene therapy, drug and growth factor delivery in a controlled fashion [32] while demonstrating a certain degree of site-specific targeting [33]. Bioactive moiety-delivery is determined by the ability of the scaffold to control and trigger the substance release in a smart manner through the interaction with bio-molecular stimuli [34]. Polymers with low molecular weight demonstrate rapid drug release, whereas high molecular weight microspheres achieve slower release [35]. Embedded within 3D scaffold as building blocks, microspheres are capable of a cumulative release of encapsulated bioactive substances [36]. Different methods such as solvent vapour treatment, solvent/non-solvent sintering, oil-in-water dispersion, selective laser sintering (SLS) are used for the production of microspheres and microsphere-based 3D scaffolds [37]. The first three methods sinter polymeric microspheres at ambient temperatures to make porous matrices for drug delivery or cell seeding. The polymerization is conducted in heterogenous (two- or multi-phase) systems where a monomer-rich phase is suspended in a solvent-rich phase. During or after polymerization, aggregation, coalescence or crosslinking of the formed microspheres/microparticles are used. The SLS is an additive manufacturing technique for fabrication of complex-shaped scaffolds without using moulds or preforms. The laser beam is the heating source for selective sintering of the powder material (metal, polymer, ceramic, composite) according to the predetermined model geometry. An advantage of the sintered porous structure is the ability to form a 3D porous structure suitable for bone regeneration [38]. For example, lovastatin microparticles in polyurethane scaffold were found to release lovastatin stimulating expression of BMP-2 growth factor in osteoblast cells in 14 days period [39] thus combining better cellular adhesion and controlled delivery of active biomolecules. However, cells could not survive as long as they are more than a few hundred μm away from blood vessels. Otherwise, gases, nutrients and soluble substances should be supplied by slow diffusion which may cause delayed new tissue formation or cell necrosis [40]. To encourage vascularization of an appropriately designed scaffold, three main approaches are applied: 1) functionalization with VEGF, 2) seeding with endothelial cells, and 3) adding angiogenic gene carrying vectors or hypoxia mimic agents [41]. Using the first approach, simultaneously loaded PLGA microspheres with BMP-2 and gelatin hydrogel with VEGF onto PP scaffold have been shown to successfully induce both enhanced bone formation and increased vascularization in rat bone *in vivo* [42].

3.4. Solid free-form scaffolds

In general, most conventional techniques for scaffold production are incapable of creating complex scaffolds with precisely controlled microarchitecture and properties [43]. 3D scaffolds with controlled architecture and reproducible properties are created by stacking CAD/CAM produced 2D shapes. After preparing 2D models, they are directly transformed into STL files and transmitted to the additive manufacturing equipment. The whole 3D scaffold is obtained by successive printing of 2D layers. The process includes precise X-Y-Z positioning system, automated material-fed system, and computer-based software for operational control. This allows high precision in spatial parameters (from mm to nm) of geometrically complex objects, controlled pore size and interconnectivity, and enhanced productivity of a wide range of biomaterials. The computer-aided method allows creating scaffolds incorporating patient-specific information in a uniquely designed micro-environment. The data for tissue geometry can derive from magnetic resonance imaging (MRI) or computed tomography (CT) that allow for reconstruction in the 3D model (reverse modelling) [44]. Derived from the 3D medical image of the defect, this fabrication technique is able to create patient-specific scaffold with the exact geometry of the defect. The individualized scaffold design provides production of more accurate and perfectly fitting implants together with decreased fabrication time. However, the accuracy of the model depends on the resolution of the device for image acquisition, 3D printing technology, and machine used.

The additive manufacturing technologies could be classified into scaffold-based (subdivided into cellular and acellular) and scaffold-free 3D printing [45]. Cellular 3D printing could be sub-categorized as extrusion-based, droplet-based, laser-based (that will be later explained), and stereolithography (SLA) while acellular printing can be sub-divided into SLS, selective laser melting (SLM), electron-beam melting (EBM), fused deposition modelling (FDM), and melt electrospinning writing [46]. SLA or vat polymerization is a process where a photoreactive resin is selectively cured while a platform moves the scaffold after each new layer is formed. The method is used for the synthesis of polymer, ceramic and polymer-ceramic composite scaffolds with high accuracy and resolution. Nonetheless, limited materials used as photoresist, residual toxic moieties, and need of post-processing remain challenges in the biomedical application of SLA scaffolds. In contrast to SLS, SLM uses a high energy density laser that completely melts the material thus increasing the mechanical strength and surface quality of the scaffold. The powders used require uniform distribution of spherical particles with equal size. The smaller the size, the higher the resolution and accuracy. When EBM is used, electron-beam gun in a high vacuum selectively scans and melts only conductive metal powder (even with high melting points) materials to form a 3D scaffold. The EBM-processed scaffolds have high surface roughness and limited accuracy [47]. FDM is an extrusion-based process that heats the material (polymer and polymer-ceramic composites) before squeezing it out of a nozzle. By moving the nozzle, the material is layer-by-layer deposited on a substrate. More comprehensive review regarding the methods of 3D scaffolds printing can be seen in Ref. [48]. Most printed scaffolds fulfil the requirements for tissue engineering applications providing interconnected micro- and macroporosity, anisotropy, and heterogeneity. Various types of materials could be used for printing of different scaffolds for skin, bone, nerve, muscle, cartilage regeneration or heart tissue replacement [49,50]. Only CAD-based design could produce scaffolds with regular and periodic structure with cube, diamond, gyroid, etc. unit cells. In that way, the porosity, pore size and surface-to-volume ratio can be exactly defined. However, biological materials should be liquidized before printing and biologically relevant cellular density is hard to be achieved [49]. Recently, the use of cryogenic 3D printing shows great potential in the incorporation of high quantity of bioactive moieties *in situ* into scaffolds. After fabrication at relatively low temperature ($-32\,°C$), high bioactivity and adequate mechanical strength without post-treatment were achieved [51]. Nonetheless, the cost of specialized equipment is still high for mass fabrication.

4. Types of 3D scaffolds based on the source material

Depending on the source of materials utilized for fabrication, 3D scaffolds could be divided into alloplastic synthetic scaffolds and natural tissue scaffolds. Even though a wide range of materials evaluated as hydrogels are commonly thought of in two groups, natural and synthetic.

4.1. Alloplastic synthetic scaffolds

Synthetically created 3D scaffolds are vastly used materials for tissue engineering since they propose almost complete control over the mechanical properties and architecture of the construct. Commonly utilized materials are metals, bioceramics, glass and glass-ceramics, synthetic polymers, and a myriad of composites. Overall, these synthetic biomaterials can be broken up into two major subgroups, non-biodegradable and biodegradable. Recently, researchers emphasize the use of biodegradable materials as they create a suitable microenvironment for growth of native tissue and are susceptible to cellular re-modelling leaving *in vivo* produced natural matrix [52]. Based on their application, the major groups of synthetic scaffold will be further discussed.

4.2. Hydrogel scaffolds

Hydrogels are composed of hydrophilic polymer chains either covalent or non-covalent (hold by intermolecular attractions) bonded. When crosslinked through either covalent or noncovalent bonds, natural (gelatin, fibrin, alginate, agarose, etc.) or synthetic (PEG, PAA, PEO, PVA, etc.) polymers form gels. In contrast to gels that are more solid-like than liquid-like, hydrogels absorb large amounts of water and swell without dissolving. In the swollen state, they are soft and elastic. The inherent crosslinking (by using bi-functional monomers) of hydrogels allows them to retain 3D shape and swell without dissolving. The higher the cross-linking extent, the lower the swelling. Both chemical and radiation crosslinkers have been used for the fabrication of hydrogels [53]. Chemical hydrogels contain covalent bonds, whereas physical hydrogels are maintained by ionic interaction, hydrogen bonding or molecular entanglement between polymeric chains. Deriving from natural macromolecules, hydrogel scaffolds exhibit high hydrophilicity, flexibility, biocompatibility, and degradability together with limited mechanical properties, the difficulty of purification and sometimes pathogen transmission and immunogenicity (depending on the source). They can be also used as injectable materials able to adapt the form of the damaged tissue. Synthetic polymers used for developing hydrogels such as PEG, PLGA, PVA, PCL, PLA, PU, etc., propose tunable and responsive physicochemical characteristics like modulus, water affinity, degradation rate, etc. at the expanse of potential cytotoxicity and lack of cell-adhesion moieties. According to their structure, both natural and synthetic hydrogels could be amorphous or semi-crystalline, while depending on their response to environmental stimuli, hydrogels could be divided into conventional and smart (intelligent). "Smart" hydrogels reversely change their swelling behaviour or structure in response to light, pressure, temperature, pH, ionic strength, electric or magnetic field, and other stimuli that make them interesting for the production of 4D scaffolds such as artificial muscles, self-regulating drug-delivery systems, etc. Hydrogels are also beneficial for cell transplantation because they offer immuno-isolation while allowing gaseous exchange as well as nutrients and metabolic substances to diffuse [54]. They are important materials for scaffolds due to the ability of tailoring the mechanical properties, including peptide moieties preventing bacterial invasion, and adhering or suspending of cells [55]. The appropriate rheological properties (dependent on hydrogel chemistry and crosslinking) of hydrogels are crucial to ensure the construct shape maintenance without compromising cell (cytocompatibility) or bioactive moiety spreading and function. Hydrogels are currently used in cell scaffolds, bone regeneration, cartilage healing, wound dress and drug or growth factor delivery [56]. The main challenge for the compatibility of hydrogels remains the toxic moieties or chemicals used in the polymerization of synthetic or crosslinking of natural hydrogel precursors, and other organic solvents, initiators, stabilizers, etc. The methods used for fabrication of hydrogel scaffolds include solvent casting/leaching, gas foaming/leaching, photolithography, electrospinning, 3D printing, etc.

4.3. Natural tissue scaffolds

Natural tissues consist of cells, growth factors and extracellular matrix (ECM). ECM is a heterogeneous hydrophilic 3D matrix that provides a proper microenvironment for cell, accumulates and presents growth factors, directs migratory cells, and participates in mechanical signalling by mechanical receptors (integrins). The composition of ECM usually includes vitronectin, fibronectin, collagen type I and II, decorin, diglycan, laminin and perlecan [57]. The main components – collagen fibres and proteoglycan (from protein and hyaluronic acid) filaments, provide the durability and tensile strength of ECM. In order to exploit the advantages of natural ECM, researchers are using the decellularization procedure to remove all cellular components that could cause an inflammatory response in the host. Thus, the remaining ECM retains its composition, architecture, integrity, biomechanical properties, biological activity, hemocompatibility and is able to direct the cell migration, tissue-specific gene expression, and to control cell fate. The process of removal of cells and their sources are crucial for the decellularized ECM (dECM) performance. The decellularized material could keep the whole organ intact or could be further processed by cutting or digesting into the liquid to form a coat or ECM-containing hydrogel. By using detergents or mechanical manipulations, natural 3D scaffolds such as heart [58], lungs [59], urethra [60] and bladders [61] are decellularized and functionalized by re-implanting host-specific stem cells (re-cellularized) together with additional growth factors [62]. The sources for creating ECM scaffolds include native devitalized and decellularized human or animal (porcine, bovine) organs and tissues or *de novo* synthesized ECM from autologous, allogenic or xenogenic cells. Usually, human samples that could be used as dECM source are either aged or diseased while xenogenic animal materials are potentially immunogenic. Moreover, difficulties in preparation could also be faced. For *in vitro* synthesis (Fig. 2) of cell-derived dECM, a proper selection of specific adult (induced pluripotent) or embryonic stem cells should be made taking into account the medical application. It was found that MSC-produced decellularized ECM dramatically increased the growth and differentiation of neural cells [63] while maintaining the multi-potentiality of MSCs during expansion *in vitro* [54]. Nonetheless, some disadvantages such as immunogenicity of material left or inhomogeneity in cell distribution may appear, and risky and long immunosuppressant treatment can be needed [64]. To avoid immunological response, autologous or allogenic sources are used. Using autologous source cells, Hang et al. produced superior urea-extracted dECM containing non-collagenous proteins enhancing MSC
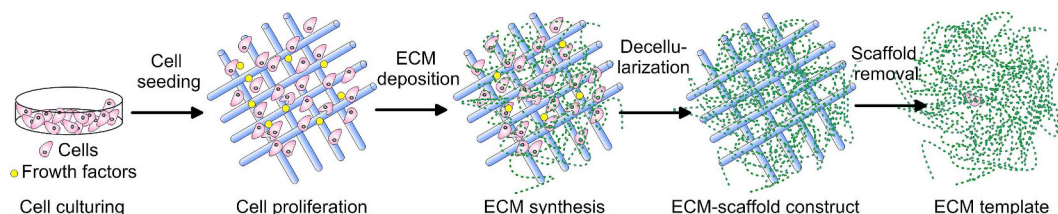

Fig. 2. Schematic overview of *in vitro* preparation of ECM template.

proliferation, migration and differentiation [65]. This strongly suggests that the origin and preparation of ECM predetermine the biological activities of biomaterial scaffolds. Additionally, different cell types could be mixed to create gradient tissue scaffolds. The cells plated in 3D scaffolds secrete and integrate new components to form ECM trying to shape their environment. Nevertheless, these artificially fabricated dECM scaffolds are less dense and have restricted chemical complexity because their organization is a result of spontaneous, rather than cell-directed polymerization [66].

Once implanted, the dECM releases soluble peptides while degrading that are able to chemo-attract stem cells to the injured sites [67]. These chemoattractive properties and degradation products vary depending on the age, species, gender or physical characteristics of ECM source. For example, a cell-derived ECM was obtained from cells grown in 3D cultures of fetal and adult synovium-derived stem cells (SDSCs) that were afterwards decellularized for ECM scaffold fabrication [68]. The fetal ECM provided a better microenvironment for proliferation, while adult ECM was advantageous for chondrogenic and adipogenic differentiation. However, all these costly and time-consuming procedures restrict the clinical application of the cell-derived matrix scaffolds.

It follows that an important factor that determines the biocompatibility of the scaffold except for the chemistry, morphology, structure, and properties, is the processing of a biomaterial. To overcome the disadvantages of a certain fabrication method, a combination of other methods could be used that complicates the existing production processes. Considering the variety of biomaterials used, not all of them are suitable for a given fabrication technology. This is a reason for constant modification of the materials which broaden their use. Since the surface characteristics such as wettability, chemistry, charge, and surface roughness are also able to regulate the contacts with the living cells and ECM proteins, a variety of surface treatments are proposed to optimize the biocompatibility of the scaffold while sealing undesirable additives and regulating absorption or corrosion rate. The next paragraphs discuss the properties, advantages and disadvantages of the major types of biomaterials used in the fabrication of 3D scaffolds dedicated for various applications.

5. Scaffolds for hard tissue application

Bone tissue consists of organic (predominantly collagen matrix, 22 wt%), inorganic (mainly HAp crystals, 69 wt%) components and water (9 wt%) [69]. In its hierarchical organization two main types of bone structures could be distinguished: trabecular (porous) and cortical (compact) bone, both reinforced with collagen fibres. Because of the natural self-repairing and regeneration ability of bones, most of the produced scaffolds aim at providing regenerative signals to osteogenic cells to enhance regeneration and repair [69]. A major difficulty in designing scaffolds for load-bearing application is to simultaneously tailor all biomaterial requirements that are competing in nature. Hard tissue scaffolds should not only be biocompatible, well-integrated with the native tissue, and easily produced but should also have an ideal replacement rate and highly porous structure which doesn't significantly compromise the adequate mechanical properties. Commonly used alloplastic synthetic scaffolds as bone grafting materials that mimic the native bone tissue and provide structural and mechanical support are metals, biomimetic ceramics and composites.

5.1. Non-biodegradable and resorbable metal scaffolds

As first-generation materials for bone substitutes, metallic 3D scaffolds are largely popular for load-bearing applications compared with ceramics or polymers because of their high mechanical strength, fatigue resistance, and printing processability. Commonly used metallic biomaterials include titanium, stainless steels, cobalt-chromium (Co–Cr) based alloys, and magnesium (Mg). Titanium (Ti) is a metallic biomaterial characterized with good biocompatibility, tensile strength, and corrosion resistance. Porous Ti scaffolds with 3D architecture benefit the vascularization, nutrient and gas transport, and cell seeding [70]. As previously explained, the pore sizes have a decisive influence on bioactivity of the porous scaffolds. In order to determine the optimum pore size, Yang et al. fabricated screw-shaped Ti6Al4V dental implant prototypes by laser beam melting (LBM) with three controlled pore sizes (200, 350 and 500 μm) [71]. MC3T3-E1 cells showed improved attachment, proliferation and differentiation on both 350 and 500 μm pore size implants. Moreover, the 350 μm pore size alloy displayed the best mechanical stress distribution in the surrounding bone under 20, 30, 40 and 80 N loading. When EBM processing was used, Ti6Al4V scaffolds revealed better anti-corrosion ability with reduced precipitates of harmful Al and V ions compared to wrought scaffolds [72]. Moreover, the same EBM technology was capable of producing double and triple-layered meshes from Ti6Al4V alloy [73]. The cylindrically shaped lattice scaffolds were composed of layers with different porosity of 65–21% in order to mimic trabecular bone structure. The graded (denser outer and less dense inner) tubular design of the scaffold demonstrated decreased Young moduli (from 0.9 to 3.6 GPa) compared with a dense alloy that brought it closer to that of human bones. By changing the morphology of the lattice structure, the deformation behaviour of the scaffold was able to provide a unique combination of high ductility, energy absorption, and strength simultaneously [73]. Nonetheless, comparing the performance of EBM-produced Ti6Al4V and Co–Cr scaffolds with similar porosity of 67–70% and pore size of 470–545 μm on bone tissue growth, Shah et al. [74] established higher osteocyte density at the periphery of Co–Cr scaffold. The authors explained that fact with the existence of more favourable biomechanical environment and higher stiffness within Co–Cr alloy as opposed to Ti6Al4V. Fousová and her group produced fully interconnected open porous scaffold with rough surface by adhering spherical particles (15–50 μm) from 316L stainless steel using SLM [75]. The mechanical properties in compression of the scaffold with square-shaped pores with size of 750 μm and porosity of 87 vol% approached those of human trabecular bone. In another study, pre-cultured cell-loaded with rat bone marrow stromal cells (BMSCs) Ti fibre mesh with volumetric porosity of 86% and fibre diameter of 45 μm demonstrated an almost complete absence of inflammatory cells and improved bone healing capacity [76]. Although the bone defect symptoms were improved, the use of embedded BMSCs requires appropriate donor sites that could cause additional pain and infection. The main problems with titanium, Co–Cr and stainless steel scaffolds remain the lack of metabolization over time, need of repeated surgery, risks of ion release and abrasion (that could trigger inflammatory cascade), disease infection, low tissue adherence and prolonged recovery time.

Porous Mg scaffolds are promising biomaterials for bone substitute application owing to their good mechanical properties and biodegradability [77]. Moreover, released Mg ions and biodegradation products in endosseous sites demonstrated the ability to induce new bone formation and neovascularization [78]. In this context, open porous Mg scaffolds with 250 and 400 μm pore size and 55% porosity were found to exhibit good cytocompatibility and enhanced alkaline phosphatase (ALP) activity indicating osteogenic differentiation *in vitro* whereas *in vivo* the scaffold with larger pore size promoted vascularization and higher bone mass formation in a rabbit model [79]. The compressive strengths were about 41 and 46 MPa whereas Young's moduli reached values of 2.2 and 2.4 GPa for 250 and 400 μm pore size scaffold, respectively which values exceeded Young's moduli of the cancellous bone. However, weak points of porous Mg scaffolds remain the fast degradation rate and accelerated micro galvanic corrosion by the presence of impurities [80,81] together with the production of a large amount of hydrogen gas during *in vivo* degradation [82]. In addition, it was found that Mg ions can negatively affect the function of red blood cells and hemolysis ratio in direct contact with blood [83].

5.2. Low degradable bioceramic, glass and glass-ceramic scaffolds

Ceramic biomaterials usually include inorganic calcium or phosphate salts that have osteoconductive (promote new bone ingrowth) and osteoinductive (promote osteoblastic differentiation) properties. Ceramics could be classified into inert (non-absorbable), semi-inert (bioactive) and non-inert (resorbable) [84]. They are commonly brittle in nature but show good compression and corrosion resistance. Hydroxyapatite (HAp, $Ca_{10}(PO_4)_6(OH)_2$), β-tricalcium phosphate (β-TCP, $Ca_3(PO_4)_2$) and bioactive glasses are among the most common biomaterials used for 3D scaffolds in bone regeneration. Except conventional methods for production of porous ceramic scaffolds such as polymer sponge method, salt leaching, dual-phase leaching, gel casting, etc., the major techniques available for ceramics 3D printing are: 1) agglomeration with polymer, chemical/physical solidification and thermal processing, and 2) sacrificial inverse matrix printing, infiltration with ceramic slurry and burning the negative [85].

Because of their similarity to bone, bio-resorbability and good biocompatibility, calcium phosphate biomaterials are widely used for orthopaedic and dental implant applications. 3D printed β-TCP scaffolds showed an increase in uniaxial strength with the increase of sintering temperature and time [86]. The compression strength could be additionally improved by controlling particle size distribution and binder's concentration. Another approach proposed by Deng at al. includes incorporation of Mn in β-TCP scaffolds that improved both biomechanical (density and compressive strength) and biological properties [87]. The ionic products from the scaffold promoted the proliferation of rabbit chondrocytes and rBMSCs *in vitro* and improved regeneration of subchondral bone and cartilage tissue as compared to β-TCP scaffolds upon transplantation in rabbit models. However, similarly to HAp, the application of β-TCP as bone regeneration scaffold is limited because of its overall poor mechanical properties. For that reason, 3D printed porous β-TCP scaffolds with interconnected squire channels (500 μm in size) were mechanically strengthened by SiO_2 (silica; 0.5 wt%) and ZnO (0.25 wt%) dopants. The cylindrical scaffolds demonstrated increased density and a mean increase in compressive strength of 250% after sintering at 1250 °C when compared to pure β-TCP scaffolds [88]. A greater rate of attachment and proliferation of human fetal osteoblast cells (hFOBCs) within the doped scaffolds was also observed.

In general, bioactive glasses (BG, $CaO–SiO_2–P_2O_5$ composition) share better degradation properties and bioactivity than HAp and β-TCP. Therefore, the biodegradation performance of ceramic bone implants could be improved by introducing mesoporous silica-based particles that also promote Si ion release known to be essential for pro-angiogenesis and healthy bone development [89]. Bioceramic scaffolds with 34% porosity were 3D printed with laser-aided gelling from $CaCO_3/SiO_2$ (5:95 wt%) sol in the form of cylindrical specimens and sintered at 1300 °C afterwards [90]. The bioceramic scaffold showed

47 MPa compressive strength value or 30% improvement over pure SiO_2 scaffold, no cytotoxicity, and good biocompatibility when tested in MG-63 osteoblast-like cells *in vitro*. Pressure extruded ceramic composite scaffolds of calcium sulphate hydrate (CSH) and mesoporous bioactive glass (MBG) with different mass ratio of the components, uniform square macroporous structure (67–68% porosity) and pore size of 350 μm indicated stimulated adhesion, proliferation and osteogenic-related gene expression of hBMSCs (human bone marrow-derived stem cells) *in vitro* [91]. *In vivo* results in rats demonstrated that the scaffolds promoted new bone formation in calvarial defects compared to pure calcium sulphate hydrate (CSH) scaffolds.

Application of growth factors or cytokines is used to promote cell differentiation, tissue formation or neoangiogenesis. On one hand, most of the growth factors (GFs) have a short half-life in circulation and on the other, fast and uncontrolled release of GFs may increase the adverse effects on non-target sites. For that reason, the controlled release of these substances is a desirable capability of the scaffold. To facilitate vascularization, Li et al. printed at room temperature (without sintering afterward) mesoporous with approximately 300 μm macropores silica/calcium phosphate cement (CPC)-based 3D scaffold with concomitant Si ion (promoting vascular tissue ingrowth) and recombinant human bone morphogenic protein-2 (rhBMP-2) release stimulating osteogenesis of human bone marrow stromal cells [92]. The produced scaffolds with uniform interconnected pore structure induced osteogenic differentiation of hBMSCs and vascularization of human umbilical vein endothelial cells (hUVECs) *in vitro*. Implanted in femur defect rabbit model abundant new vessels around the complex scaffold and rapid rate of osteogenesis were observed as compared to CPC control scaffolds [92]. Moreover, various studies demonstrated improvement in biological and physicochemical properties of mesoporous bioactive glass (MBG) scaffolds by incorporation inorganic therapeutic components such as Sr [93], Zn, Mg [94,95], Zr [96], Ga [97], or B [98]. Incorporation of beneficial Fe (5–10%) in MBG turned the scaffolds with high porosity (83%) into biocompatible magnetic material that exposed to the external magnetic field had great potential for use in hyperthermia therapy (at around 43 °C) of malignant bone tumours [99]. The scaffolds with a hierarchical structure of large 300–500 μm pores and 4.5 nm mesopores demonstrated a slight decrease in compressive strength (46–48 kPa) as opposed to pure PBG scaffolds (50 kPa). The multifunctionality of Fe-MBG scaffolds that makes them suitable for therapy of malignant bone diseases is schematically presented in Fig. 3. Five percentage of Fe in MBG scaffold benefited the mitochondrial activity and gene expression of BMSCs indicating improved osteoconductivity of the implant. This fact the authors explained with changes in ionic composition and pH value that improved cell viability and differentiation [99]. Moreover, mesoporous silica displayed additional capability of local drug release owing to its large nanopore volume, size and surface area. To demonstrate that Zhang et al. fabricated
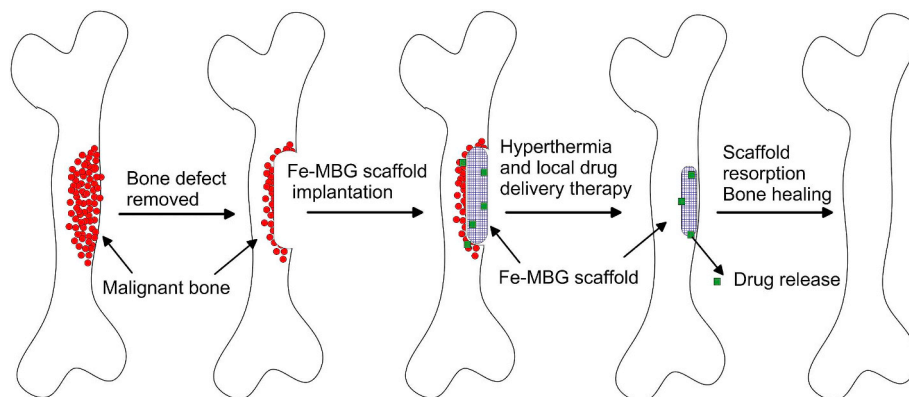

Fig. 3. A scheme illustrating the potential application of Fe-MBG scaffolds for malignant bone treatment (hyperthermia) and regeneration of the defect bone. Adapted from Ref. [99].

3D printed porous Sr-containing MBG porous (400 μm pore size, 70% porosity) scaffold that showed sustained dexamethasone (anti-inflammatory drug) release with a rate depending on Sr dissolution characteristics of the scaffold [100]. To combine drug-delivery properties with additional angiogenetic and antibacterial properties, multifunctional Cu-containing MBG scaffold with large pore size of 300–500 μm loaded with ibuprofen was prepared by simple polymer sponge method [101]. The ion (Cu^{2+}) release was able to induce a hypoxic cascade of hBMSCs activating neovascularization, promote osteogenic differentiation, and prevent osteomyelitis incidence by infections. In this respect, composite ceramic scaffolds could meet all the requirements of a bioresorbable therapeutic cell and drug (or antibiotics and growth-factors) carriers for improved healing in bone tissue engineering. The major disadvantages of ceramic scaffolds are their brittleness, compressive strength lower than that of the human bone (100–230 MPa [102]) at high volume percentage of porosity, and the need of high sintering temperature that limits the incorporation of bioactive molecules in the scaffolds. Some ceramics such as calcium sulphate hydrates (CSH) display faster degradation rate than the formation of new bone and a release of acidic degradation products that are not beneficial for cell proliferation and viability [103]. Other ceramics like wollastonite ($CaSiO_3$) are difficult to be cut and shaped in uniform porous scaffold with controllable mechanical properties and porosity [104]. Moreover, the highly promising MBG scaffolds could have high degradation rate together with unstable interface/surface performance that could also decrease cell attachment and proliferation.

5.3. Polymer scaffolds

Polymer materials are vastly used to renovate the traumatized tissue due to their unique properties such as biocompatibility, reproducible mechanical, physical properties, workability, and low price. Because non-biodegradable synthetic polymer scaffolds require a procedure of surgical removal, they are not widely used. Some acrylic polymers like PHEMA, PHPMA, PMMA [105,106], and conductive polymers [107] are such representatives. Two-part self-polymerizing PMMA cement is known to be the most enduring material in orthopaedic surgery used in total joint replacement for fixation of components [108]. However, drawbacks such as aseptic loosening caused by monomer-mediated bone damage, inherit inert properties, and mechanical mismatch during long term wearing are also reported [108].

Biodegradable polymers with tunable degradation rates could be both natural (from human or animal tissues) and synthetic. Their degradation rate depends on molecular weight, the structural arrangement of macromolecules (amorphous/crystal structure), isomeric characteristics, formulation, architecture, and quantity of the material [109–151]. Natural polymer scaffolds usually demonstrate a lack of immune response and better cell interactions while synthetic polymers are cheaper, stronger, and have better functionality although sometimes triggering immune response and toxicity [37]. Biodegradable polymers demonstrate suboptimal load-bearing capacity when used alone that limit their application as hard tissue scaffolds. However, in pulpodentinal complex and periodontal apparatus, the smaller sizes and difficulties in reaching the target places require soft, injectable scaffolds that match irregular patient defects [110]. Moreover, the ability of polymers to incorporate diverse bioactive moieties could be most eminent to induce osteogenic differentiation in less loaded constructs. For example, immobilizing or including GFs within the scaffold are promising approaches as many GFs exhibit inherited binding properties to molecules of ECM through specific binding protein intermediaries [111]. Bilayer system of porous PLGA cylinder overlaid with PLGA microspheres dispersed in alginate sponge matrix was examined for localized delivery of pre-encapsulated transforming growth factor-β1 (TGF β1 – 50 ng) and bone morphogenic protein-2 (BMP-2 – 2.5 and 5 μg) applied for osteochondral defect repair [112]. *In vitro*, the total dose of GFs was delivered at the end of the sixth week. After co-encapsulation of TGF-β1 with a higher dose of BMP-2, the histological analysis demonstrated tissue repair after very short (2 weeks) period, higher quality cartilage with improved surface regularity, and very good tissue integration in the rabbit model. The controlled release rate of GFs from the scaffolds preserved cartilage integrity from 12 to 24 weeks [112]. Using non-biodegradable orientated in parallel arrays of polystyrene sub-micron fibres with diameter (630–760 nm) approximating the diameter of ECM fibres, coated with fibrin and bioprinted with tendon- or bone-promoting-GFs (fibroblast growth factor-2 (FGF-2) or BMP-2, respectively), Ker et al. [113] inhibited the myocyte differentiation of mouse C2C12 myoblasts and stimulated cell alignment, tenocyte and osteoblast differentiation. The bioprinting technique gives the possibility to have direct control over the concentration of the immobilized growth factors. Therefore, using hydrogel with embedded GFs, it is possible to present a precise quantity of extrinsic factors and direct cells rather than adding them in the culture medium.

5.4. Particle loaded polymeric and other composite scaffolds

The development of composite scaffolds allows for the engineering of biomaterials with suitable mechanical and physiological properties by controlling the type, size, fraction, morphology and arrangement of the reinforcing phase. Moreover, the degradation behaviour of the scaffolds could be altered by adding bioactive phase in the matrix [114]. For instance, PCL is relatively elastic and drug permeable but has poor mechanical stability (low modulus with high elongation behaviour), slow degradation (2–4 years) in living tissue, and poor cellular adhesion properties. However, it shows blend compatibility with other biomaterials such as Sr-hydroxyapatite [115], nanohydroxyapatite, nanocellulose, carbon nanotubes [116,117], cyclodextrins [118], etc. It follows that PCL possesses the capacity for functionalization while overcoming the poor mechanical stability and low bioactivity of the unmodified polymer. PGA/HAp composites demonstrated high bioactivity, osteoconductivity uniform cell seeding, cell ingrowth and tissue formation as hard tissue scaffolds [119]. By releasing Ca and Si ions, MBG powders were also found to neutralize the acidic degradation of synthetic polymers such as PLGA in composite scaffolds and stimulate thereby cell response [120]. The ceramic mesoporous powders increased hydrophilicity, water absorption and degradation rate of the composite compared to pristine PLGA scaffolds. Electrospun hybrid scaffolds of randomly orientated fibres (average diameter 4.11 μm) of poly (3-hydroxybutyrate-*co*-3-hydroxyvalerate) and silicate containing hydroxyapatite nanoparticles (PHBV-SiHAp) seeded with hMSCs showed the largest adhesion and differentiation ability compared with pure piezoelectric PHBV and non-piezoelectric PCL scaffolds [121]. The composite scaffold revealed improved mineralization and superior osteoinductive properties either because of changed scaffold chemistry by the presence of bioactive SiHAp nanoparticles or by altering scaffold charge due to inherited piezoelectricity of PHBV.

In another study, calcium phosphate cement (CPC)-based scaffold incorporating chitosan, absorbable fibres, and hydrogel microbeads possessed 4-fold increased flexural strength and 20-fold enhanced toughness compared to rigid CPC microbead scaffolds which matched the strength of cancellous bone [122]. These non-rigid scaffolds demonstrated excellent proliferation, osteodifferentiation and enhanced mineralization when incubated with human umbilical cord mesenchymal stem cells (hUCMSC) *in vitro*. Similarly, freeze-dried porous fluorhydroxyaptite (FHAp)-Mg-gelatin scaffold with different amount of FHAp (30, 40, 50 wt%) and pore size of 150–250 μm improved the compressive strength of the polymer from about 2.1 MPa to 3.3 MPa at the highest amount of FHAp and supported the proliferation and adhesion of MG-63 cells for bone regeneration [123]. Graphene alone was found to stimulate osteogenesis [124] while covalent associations of graphene oxide (GO) flakes (4 nm thick) in porous collagen scaffolds directed the stem cells fate toward osteogenic differentiation by upregulating cell-adhesion molecules and stiffening the scaffold [125]. As

Table 2
Composite scaffolds for bone tissue application.

Biomaterial composition	Fabrication	Cell type	Outcome	Ref.
Gelatine, alginate, HAp scaffolds	Extrusion	hMSCs	Cell survived the printing process and showed 85% viability after 3 days	[134]
Chitin-nanoHAp scaffolds	Freezing/thawing method	COS-7 (fibroblast-like) cell line	Good adhesion and proliferation of cells	[135]
Gelatin-carboxymethyl chitosan-nanoHAp scaffolds	High stirring-induced foaming and freeze-drying	Human Wharton's jelly-derived mesenchymal stem cell microtissues	Cell growth, proliferation and differentiation; high mineralization capacity	[136]
Glycol chitosan-hyaluronic acid-nanoHAp scaffolds	Injectable	MC-3T3-E1	Cytocompatibility with cells well attached to the pores	[137]
Chitosan, gelatin, and GO containing scaffolds	Freeze-drying	Rat calvarial osteoprogenitor cells and mouse mesenchymal stem cells (C3H10T1/2)	Promote differentiation into osteoblasts; increased collagen deposition in vivo	[138]
Chitosan-nanoHAp containing Cu/Zn alloy nanoparticle scaffolds	Freeze-drying	Rat osteoprogenitor cells	Increase protein adsorption and antibacterial activity; no toxicity towards osteoprogenitor cells	[139]
Blended PLGA-silk fibroin fibrous scaffold coated with HAp	Electrospinning	MSCs	Increased adhesion, proliferation and differentiation towards osteoblasts; excellent cytocompatibility and good osteogenic activity	[140]
Micro-nano PLGA-collagen – nanoHAp rods scaffolds	Electrospinning	MC3T3-E1	Improved osteogenic properties; bioactivity	[141]
Alginate-PVA-HAp hydrogel scaffold	Bioprinting	MC3T3	Excellent osteoconductivity; well distributed and encapsulated cells	[142]
Tri-layer scaffold consisting of superficial PVA/PVAc-simvastatin (a type of statin)-loaded layer, followed by PLC-cellulose acetate-β-TCP layer and final PCL layer	Electrospinning	MC3T3-E1	Higher mineralization; enhanced cell attachment and proliferation	[143]
Laminated nanoHAp layer on PHB (polyhydroxybutyrate) fibrous scaffold	Electrospinning	MSCs	Better adherence, proliferation and osteogenic phenotype formation	[144]
PMMA-nHAp decorated cubic scaffold	Solvent casting and particle leaching	MG-63	Friendly environment for cell growth and protection from microbial infection	[145]
PLGA/TiO$_2$ nanotube sintered microsphere scaffolds	Emulsion and solvent evaporation method and sintering	G-292 cell lines	Increased cell viability; a higher amount of bone formation	[146]
PU fibrous scaffolds loaded with MWCNTs (0.4 wt%) and ZnO nanoparticles (0.2 wt%)	Electrospinning	MC3T3-E1	Scaffolds promote osteogenic differentiation	[147]
PCL-nanoHAp nanofibre layer deposited on Mg alloy scaffold	Electrospinning	Osteocytes	Retard corrosion and increased osteocompatibility; higher cell attachment and proliferation	[148]
Porous rGO-nanoHAp scaffold	Self-assembly	rBMSCs (rat bone mesenchymal stem cells)	Enhanced proliferation and osteogenic gene expression	[149]
PLLA - osteogenic dECM (from MC3T3-E1) scaffolds	Electrospinning	mBMSCs (mouse bone marrow stem cells)	Faster proliferation; early stage osteogenic differentiation	[150]

opposed to pure collagen scaffolds (14.6 kPa), GO-collagen construct showed elastic moduli of about 39 kPa. It was also demonstrated that adding silk (2.5 and 5 wt%) to mesoporous bioactive glass (MBG) scaffold (94% porosity) improved its mechanical properties, cell attachment, proliferation and controlled drug release [126]. The compressive strength rose up from 60 kPa up to 250 kPa when incorporating 5 wt% silk in MBG scaffold which means 300% increase. The degradation rate of the composite was slower as opposed to that of a MBG scaffold and a thin silk film on the pore walls (200–400 μm pore size) was formed. Thus formed stable surfaces with fibroin provided better support for BMSCs proliferation and differentiation [126].

In a remarkable study, Cheng et al. tried to construct highly porous bilayer scaffold with interconnected honeycomb structure with chondral (consisting of plasmid TGF-β1-activated chitosan-gelatin scaffold) phase integrated into osseous (of plasmid BMP-2-activated HAp/chitosan-gelatin scaffold) phase [127]. This bilayer gene-activated scaffold with pores of about 50–100 μm was dedicated to spatial control of localized gene delivery that could induce the mesenchymal stem cells in different layers to differentiate into chondrocytes and osteoblasts *in vitro* and *in vivo*. The spatially controlled and sustained delivery of plasmid DNA encoding for tissue inductive factors maintained the specific cell phenotypes of complex osteochondral integrated tissue derived from a single stem/progenitor cell source *in vitro*. *In vivo*, the complex scaffold gave simultaneous support of articular cartilage and subchondral bone [127].

The surface properties of 3D scaffold biomaterials could be altered in order to promote their bioactivity, corrosion resistance, hydrophilicity, mechanical strength or tribological properties. For example, bioactive adhesive molecules such as collagen, fibronectin, growth factors, insulin, etc. can be covalently or physically attached on the biomaterial surface. These modified 3D scaffolds are able to modulate in a complex fashion the cellular response. Such hybrid polymeric-bioceramic porous (over 60% porosity) scaffolds of β-TCP/HAp vacuum coated with alginate demonstrated improved osteoblast adhesion, maturation and proliferation as well as an enhanced mechanical performance involving increased fracture toughness, Young's modulus, and compressive stress close to that of cancellous bone [128]. The improved osteoblast adhesion and migration the authors attributed to the additional biocompatibility created by alginate via changing surface microtopography and roughness. Another approach aiming at increasing the bioactivity and biocompatibility of metal implants is deposition of wollastonite ($CaSiO_3$) [129], calcium phosphate [130], biomimetic nanoapatite [131], or polycrystalline diamond [132] coatings on different titanium scaffolds. When EBM-manufactured Ti6Al4V scaffold was functionalized with Ag and CaP nanoparticles via electrophoretic deposition, the change in hydrophobicity and surface roughness at nanoscale provided physical cues that disrupted bacterial adhesion [133]. The silver nanoparticles at concentration 0.02 mg/cm^2 in CaP film covered with positively charged PEI indicated bacteriostatic activity against gram positive bacteria, *S. aureus,* during 17 h of exposition. Although bi- and multiphasic scaffolds provide enhanced

mechanical and biological performance, there is always a concern about the adhesive strength between the adjacent layers or contacting non-homogeneous biomaterials that could lead to delamination or crack propagation. Although improving the surface performance, these additional modifications are usually cost- and time-consuming.

A summary of recent studies on composite scaffolds using numerous production technologies and stem cells dedicated to a hard tissue application is reported in Table 2.

6. Scaffolds for soft tissue application

By careful selection of biomaterials and key scaffold characteristics, researchers developed novel techniques for developing complex architectures with desired properties for soft-tissue engineering applications. These scaffolds should be fabricated so that to regenerate and mimic both the anatomical structure and function of the original soft tissue to be repaired. Polymers are commonly used biomaterials to construct soft matrices that are widely utilized for the production of most of the transplanted organs such as kidneys and liver [2], but also successfully applied for muscles, tendon [151,152], heart valves, arteries [153], bladder and pancreas [154,155] regeneration.

6.1. Synthetic polymer scaffolds

Synthetic polymers are easily produced under controlled conditions. Their physical and mechanical properties are tunable, predictable and reproducible and thus, could be tailored for the production of scaffolds dedicated for a specific application. The most commonly utilized synthetic polymer for drug, gene, and growth factor delivery application [156–158], is PLGA, a flexible and permeable copolymer of lactic and glycolic acid. Each lactic acid residue includes a pendant methyl group which makes the surface hydrophobic. The polymer chains show a lack of functional groups and biodegrade in non-toxic but highly acidic glycolic and lactic acid [159]. To address the problem with acidity, a greater amount of glycolic than lactic acid could be used to form PLGA that lessens the degradation rate and lowers the acidic byproducts. Because of their semi-permeability, PLGA microspheres were used to entrap living cells like myoblasts [160]. When subcutaneously implanted, the former simultaneously released therapeutic anti-inflammatory drug to protect these cell from the host immune system (Fig. 4). The myoblast cells retained their viability in 30 day period suggesting that the semi-permeable microspheres allowed appropriate diffusion of nutrients and oxygen. These encapsulated cell implants loaded with dexamethasone, after 60 days of subcutaneous post-implantation in rats diminished the inflammatory response by sustain delivery of the drug. The histological analysis revealed that blood capillaries surrounded the microcapsule aggregates in 100 μl dexamethasone-treated mice group [160].

Not only encapsulated but also aligned nanofibre scaffolds were found to be suitable for highly organized soft tissues such as skeletal muscle, ligament and peripheral nerve regeneration whereas random
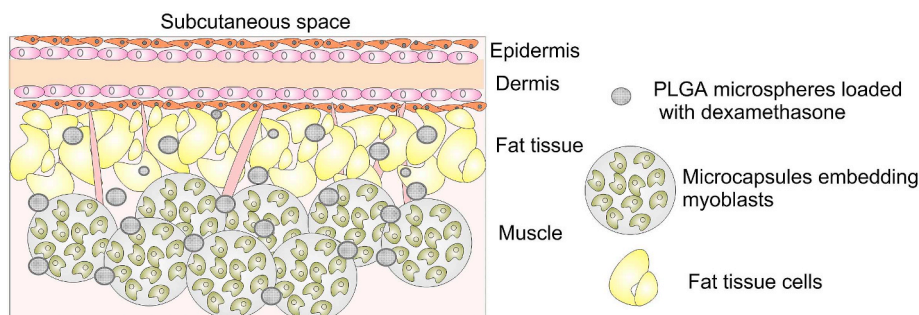

Fig. 4. Schematic representation of subcutaneous microenvironment after implantation of encapsulated myoblast cells and microspheres releasing dexamethasone in mice. Adapted from Ref. [160].

nanofibres were useful for cartilage and skin regeneration application [161]. Since muscle fibres must grow parallel to one another following identical anisotropy, electrospun PLGA scaffolds of aligned fibres with a diameter of about 0.6–0.9 μm were found to provide topographical cues guiding the alignment of myoblast cells (C2C12 murine myoblasts) and encouraging their differentiation as compared with randomly oriented fibre substrates [162]. Moreover, the incorporation of polyaniline in PCL well-ordered fibrous scaffolds increased the electrical conductivity of constructs thus giving not only topographical but also electrical cues to C2C12 myoblast cells both synergistically improving myotube maturity [163]. Another approach applied is using permeable core-shell nanofibres that incorporate bioactive agents and enable controlled release within the tissue. The active substance is usually entrapped in the core layer. Li et al. used co-axial electrospinning where two syringe pumps fed both solutions separately (Fig. 5) to produce poly(L-lactide-co-ε-caprolactone), (PLC) fibrous scaffold of different LA:CL ratio and BSA (model protein) containing core, namely PLC(50:50)BSA and PLC(75:25)BSA [164]. The BSA release of PLC(50:50)BSA and proliferation rate of hMSCs toward smooth muscle cells were higher than those of PLA(75:25)BSA. Except for tunable mechanical properties, these core-shell nanofibres possessed regulable release potential as medical 3D scaffolds.

Damaged neural tissues are known to regenerate for a longer period of time whereas sometimes larger nerves never recover. Similarly to muscle scaffolds, for enhanced nerve regeneration fibrous scaffolds of PLLA, PCL, PGA, etc. with aligned or random arrangements are commonly used [165]. Moreover, different studies demonstrated that therapeutic cell-laden scaffolds also enhanced *in vivo* soft tissue regeneration. For example, by combining longitudinal aligned electrospun scaffolds of PCL and PLGA (proportion of 4.5:5.5) with hDFCs (human dental follicle cells), neural regeneration was stimulated [166]. The authors found no cytotoxic reactions and when transplanted to restore the defect in rat spinal cord, re-myelination and induced tissue polarity occurred. It was also reported that incorporating of nerve growth factor (NGF) into aligned core-shell PLGA nanofibres enhanced physical and biomolecular signalling and promoted better nerve regeneration in 13-mm rat sciatic nerve defect than only PLGA scaffold [167]. Similarly, a strong electrospun fibre-aligned scaffold of PCL and PLLA with incorporated bFGF and PGF (platelet-derived growth factor) was found to up-regulate the gene expression of hMSCs *in vitro* [168] critical for the viability and repair of the anterior cruciate ligament that had a poor healing capability.

The complexity of mechanical requirements and physical properties of cartilage hinders the fabrication of effective artificial scaffolds for cartilage regeneration. Because of low coefficient of friction (0.02–0.05

against smooth and wet substances), high permeability to fluids, and biocompatibility, PVA-based hydrogels were developed to be used as synthetic scaffolds for articulating cartilage [169]. Kim and his group developed macroporous PVA sponge incorporating in its pores encapsulated rabbit chondrocytes in photocrosslinkable PEG derivates that improved *in vitro* chondrocyte functions and collagen accumulation within the scaffold [170]. In an ectopic mouse model, the mechanical properties of the cell-laden PVA-based scaffold were biomimetically reinforced by over 80% compared to their acellular counterparts. Similarly, by encapsulating chondrocytes in a photopolymerized degradable PEG tiol-ene hydrogel scaffold with localized presentation of TGF-β1, Sridhar et al. demonstrated *in vitro* cell viability, proliferation, and cartilage-specific molecules generation at a higher rate than without GF [171]. It follows that tethering GFs into synthetic polymer scaffolds integrates promoting effect on cells and provides advantages for clinical applications. An issue when using extrusion printing technology for scaffold production is the elevated temperature (above 100 °C) that prevents the incorporation of bioactive materials promoting the healing process. Guo et al. proposed lowering the printing temperature of PLGA scaffold by utilizing dimethyl sulfoxide (DMSO) as a solvent that allows for the incorporation of proteins favourable for induction of hMSC differentiation [172]. After the solvent treatment, the material became tougher with improved flexibility and compressive strength similar to that of native cartilage while the activity of the growth factors was retained with the cold printing method used.

In another study, thermoplastic polyurethane (TPU) (25%)/PCL (75%) blends with thermally induced shape memory were produced by melt blending and showed 98% shape fixing ratio and 90% shape recovery ratio upon heating (60 °C in hot water bath). 3T3 fibroblasts cells cultured on the TPU/PCL scaffold indicated high viability together with obvious cell-substrate interactions [173] that make the composite biomaterial suitable for surgical sutures or other medical devices. However, many synthetic polymers demonstrate low cell-affinity surfaces [174], hard to control degradation rate, and *in vitro* cytotoxicity [159]. Other problems encountered are lack of hydrophilicity, bioactivity, and release of acidic by-products that lower pH values and trigger inflammatory response [175].

Synthetic supramolecular scaffolds are also applied in regenerative medicine. Synthetic peptides usually form a network of waving nanofibres with a diameter of around 10 nm. They successfully mimic the native microenvironment of ECM because of their biomechanical properties and nanoscale network. Self-assembly synthetic peptide-based hydrogels are attractive candidates for scaffold materials showing biocompatibility and ability to attach versatile chemical groups. They also demonstrate hypo-immunogenicity, slow degradation (by
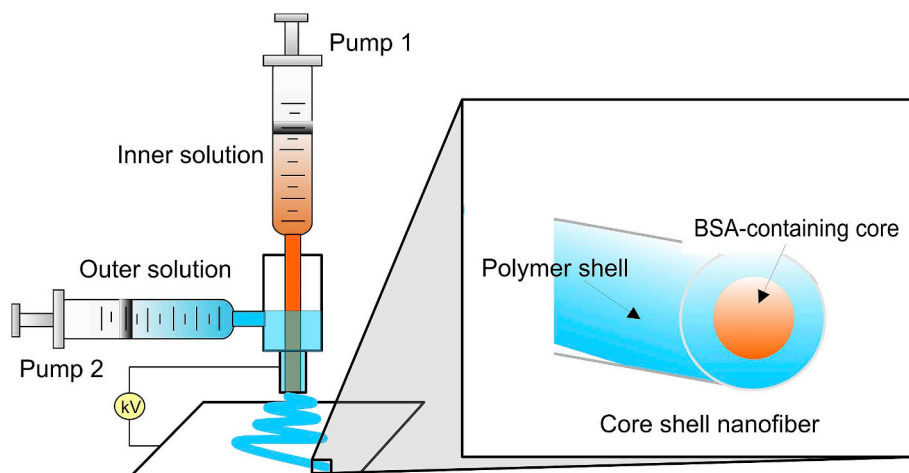

Fig. 5. A scheme illustrating the principle of co-axial electrospinning where the polymer in a solvent coats the inner aqueous solution while immerging from the needle. As a result, a smooth and beadless core-shell nanofibre is formed. Adapted from Ref. [164].

proteases), and sustained release of different bioactive moieties immobilized by covalent or non-covalent bonds to the peptide chains. Moreover, without additional external growth factors, synthetic glycosaminoglycan (GAG) mimetic peptide nanofibre scaffolds were found to be able to induce neovascularization and cardiomyocyte differentiation for the regeneration of cardiovascular tissue in mice [176]. The GAG-mimic scaffold increased the VEGF expression and localization in the ischemic area and was able to induce activation and migration of cardiac stem cells. Peptide nanofibres were also used to transplant pancreatic islets with improved both numbers of instrumental vessels and viability of islets in diabetic rats [177]. A glucosaminoglycan – heparin, shows growth factor- (such as VEGF, FGFβ, TGFβ1) and cell surface receptor-binding affinity. For that reason, it was used in constructing self-assembling peptide (RAD16-I)-heparin fibrous hydrogel scaffold that was found to improve cell survival and differentiation of cells undergoing chondrogenesis probably because of clustering of receptors in the presence of growth factors associated to ECM and, therefore, signalling to the receptors [178]. The potential of these synthetic biomaterials lies in the variability in composition, peptide length and scaffold design. Because of their low mobility and high viscosity, self-assembling peptides are mostly used for local protein, gene, drug, etc. delivery [179]. Nonetheless, the control over the length and structure of supramolecular is a great challenge influencing their application and biomedical safety. Additionally, it is hard to consider the effects of different combinations of peptides on binding ability with other molecules and the motif (amino acid sequence with a specific function) design assembly on functionalization and expectable bio-properties of the peptide sequence.

6.2. Natural polymer scaffolds

Natural polymers are biodegradable and bioactive materials that can be classified into proteins, polysaccharides and polynucleotides (Table 1). As the main protein in ECM, collagen 3D scaffolds are widely used in cartilage [180], vasculature [181], nerve [182,183], and muscles [184] regeneration. Without additional modification, collagen hydrogels display the intrinsic ability of biological recognition such as receptor-binding ligand presentation and susceptibility to cell-triggered proteolytic degradation. The basic molecular unit of collagen is tropocollagen containing triple helix structure. It is the most abundant protein (25–35% of the total body content) in ECM of various connective tissue in the human body [185]. When honeycomb collagen sponge scaffolds containing bone marrow stromal cells (BMSCs) were implanted into rat model, better sensory and motor recovery of dorsal root ganglion than only honeycomb scaffold was observed [186].

Chitosan is a polysaccharide compound derived from partial deacetylation of chitin extracted primary of shellfish sources. Self-healing chitosan-based hydrogel scaffolds with 1.5 kPa stiffness demonstrated *in vivo* proliferation and differentiation of neuro-progenitors in the central nervous system of Zebrafish model [187] which made them also suitable for neuro-regeneration. To facilitate cellular attachment, spreading, proliferation, and cytoskeletal organization a successful approach is to incorporate integrin-binding peptide sequence such as RGD (arginine-glycine-aspartic acid) in natural hydrogel scaffolds [188]. The pro-inflammatory fibrinogen that is a natural polymer, contains multiple cell-binding motifs including RGD. Zaviscova et al. examined the neurogenic potential of RGD-modified (20 mg/mL) hydroxyphenyl derivate of HA-based hydrogel (HA-PH-RGD), fibronectin-modified HA-PH-RGD (HA-PH-RGD/F), and HA-PH-RGD/F combined with mesenchymal stem cells (MSCs) and found out that after injection of HA-PH-RGD and HA-PH-RGD/F in rats the density of neuro-filament fibres in the leisure increased and neo-vascularization was supported while these effects were further increased by adding MSCs to HA-PH-RGD/F [189]. These transplanted cells released trophic factors that provided immunomodulatory and lasting neurotrophic effect. When combining chitosan with pro-inflammatory fibrinogen the scaffolds stimulated

adhesion of natural killer cells [190] that are responsible for activation of stem cell migration.

The good gelling properties of alginate (polysaccharide extracted from brown algae) allow the polymer to be used as an injectable scaffold for damaged cartilage repair. When human dental pulp stem cells cultured in 3% alginate hydrogel were implanted in a rabbit cartilage defect, significant cartilage regeneration was observed after 3 months [191]. Suitable not only for cartilage [192] and tendon [193] regeneration but also for wound dressing application [194] is silk fibroin, a protein distinguished by its high tensile strength and enhanced cellular adhesion properties. Hyaluronic acid (HA) is a linear polysaccharide that is one of the most important constituents of ECM. Due to the encapsulating and swelling capability of HA, it is used for delivery application [195] whereas porous HA scaffolds assembled by layer-by-layer spray assisted method demonstrated enhanced *in vitro* human keratinocytes adhesion and proliferation [196]. However, native HA does not support cell adhesion and its functional groups need to be chemically modified. In contrast, keratin is a family of fibrous proteins containing cell adhesion RGD sequences similar to fibronectin. In the form of 3D scaffolds produced by lyophilization method, keratin supported hADSCs adhesion, proliferation, and differentiation and the constructs were proved to shorten wound healing time and accelerate epithelialization *in vivo* [197]. Gelatin is a biopolymer product of either partial acid or alkaline hydrolysis of animal collagen. Gelatin scaffolds showed good affinity to human dermal fibroblasts that made them suitable for skin regeneration scaffolds [198] while the high viability of hUVSMCs (human umbilical vein smooth muscle cells) cultivated on gelatin nanofibre scaffolds indicated a high potential for muscle regeneration [199]. However, disadvantages of natural polymer scaffolds are weak biomechanics, low stiffness [200], inappropriate degradation rate with tissue regeneration rate, high price, and lack of surface specificity. Additionally, some natural materials may incite inflammation in body right [201]. Most natural polymers exhibit good biocompatibility together with poor processability.

6.3. Natural-synthetic polymer blends and composite scaffolds

On one hand, the poor mechanical properties incapable of maintaining the desired 3D shape of scaffolds comprising only of natural hydrogels is a critical issue. There was found an inverse relationship between degradation rate and mechanical strength. On the other, synthetic polymers show low cell affinity due to hydrophobicity and lack of cell recognition sites but they have high flexibility in modification. For that reason, combinations of natural and synthetic polymers have been used to design scaffolds with enhanced biodegradability, cell attachment, and hydrophilicity [202]. For example, solid-state synthetic thermoplastic biopolymers such as PCL and PLGA could be dispensed together with natural hydrogels with or without different cells seeding. Shim at al. proposed manufacturing of enhanced 3D bioprinted constructs from PCL and alginate (4% w/v) where PCL acted as mechanically stable framework whereas alginate was responsible for the real tissue cell arrangement [203]. The dual cell-laden (osteoblasts and chondrocytes) scaffold enabled viability and proliferation of printed cells while retaining their initial position which is important for the regeneration of anatomically complex such as osteochondral tissues. In another study, chitosan microparticles (10 and 20 wt%) that naturally promote cellular adhesion without additional functionalization, were used for blending of the porous scaffolds with 10 and 15 wt% PCL [204]. 10 wt% PCL with 10 wt% chitosan improved not only storage and loss moduli but also the *in vitro* production of type II collagen by chondrocytes.

Electrospun microfibrous scaffold from collagen/hyaluronic acid-based poly (L-lactide-*co*-ε-caprolactone)/PLC (9.5/0.5/20 w/w/w) demonstrated higher water uptake and lower Young modulus as opposed to control PLC scaffold that made it suitable for clinical wound healing applications [205]. The complex scaffold better supported the adhesion

of human umbilical vein endothelial cells (hUVECs) and adipose tissue-derived mesenchymal stem cells (ADMSCs) and led to 1.6 fold increase in total vessel length than pure PCL scaffold. Similarly, bilayer electrospun scaffolds of outer gelatin and inner keratin nanofibres (~160 nm) with random arrangements on PU dressing enhanced fibroblast proliferation in contrast to gelatin mat [206]. The bilayer scaffold promoted earlier vascularization and better wound healing capacity. Other complex scaffold composed of hyaluronic acid hydrogel with multi-tubular conformation modified with *anti*-Nago receptor antibody and mixed with PLGA microspheres loaded with brain-derived neurotrophic factor and VEGF displayed very good biocompatibility, anti-inflammation activity, spinal repair, and enhanced blood vessel formation when implanted in rat [207]. Table 3 summarizes recent studies on polymer blends used for various soft tissue applications together with their production technologies and stem cells tested.

When soft tissues require high mechanical activity like cartilage, heart valves, blood vessels, or dermis, the scaffold ought to have sufficient strength which is important for the effective transfer of mechanical stimuli [226]. As demonstrated previously, incorporation of bioactive particles in polymer constructs can influence the mechanical behaviour, degradability and biological performance of composite scaffolds. Freeze-dried porous collagen (70 wt%)/HAp (30 wt%) scaffolds with average pore diameter of 147 μm and 89% porosity outperformed the mechanical and osteoconductive properties of individual HAp and collagen scaffolds which make them potential candidates for the regeneration of damaged cartilage tissue [227]. Similarly, it was reported that PLGA/nanoHAp scaffolds substantially improved the cartilage regeneration as compared with pure PLGA scaffold [228]. Nano-GO (1 mg/ml) incorporated into a gelatin-based matrix that after stereolithography printing photopolymerized into the hierarchical scaffold with pores of around 200 μm, demonstrated higher compressive modulus and induced higher cell proliferation and chondrogenic differentiation of hMSCs when compared to those without GO [229]. Although the reinforced scaffolds achieved load-bearing properties similar to those of cartilage tissue, the hydrogel containing composites may not be sufficiently stable and their degradability rates should be further examined.

Additionally, by incorporating various substances, scaffold materials can be modified or functionalized not only to increase material for hosting the cells but also potent anti-inflammatory activity. In this respect, polyurethane (PU) nano-fibrous scaffolds that could be prepared in both degradable (suitable for skin tissue engineering) and non-degradable (appropriate for wound dressing application) forms were blended with antimicrobial substances such as silver nanoparticles [230], copper oxide (showing additional angiogenesis activity) nanoparticles [231], and antibiotics [232]. Simultaneously, these scaffolds showed low toxicity towards both keratinocytes [230] and fibroblasts [231] which make them viable candidates for clinical wound healing application. Moreover, electrospun composite poly(acrylic acid) (PAA) nanofibre scaffolds incorporating reduced GO (rGO) exhibited controlled near-infrared photo-thermal release of pre-loaded antibiotics (ampicillin and cefepime) with release rate depending on the applied radiation [233]. The nanofibre platform demonstrated the ability to be re-loaded with antibiotics indicating recyclability and stability. The *in vivo* studies on *S. aureus* infected mice showed excellent would healing capability making the scaffold a suitable platform that could be adapted for on-demand delivery of different drugs.

7. Cell-laden scaffolds

Bioprinting allows obtaining pre-determined 3D architectures from living multi-potent cells or ECM components that can grow for later implantation. To maintain the viability of the cells, additional growth and differentiation factors have to be added to the construction so that all components analogous of living tissue (cells and ECM) to be generated. During printing, the biomaterial behaves like a liquid that could

Table 3
Examples for scaffolds of polymer blends with soft tissue application.

Biomaterial composition	Fabrication	Cell type	Application	Ref.
Collagen and fibrinogen scaffolds	Inkjet printing	Chondrocytes	Cartilage	[208]
Gelatin and fibrinogen scaffolds	Extrusion	hMSCs, hUVECs, hNDFs	Vascular	[209]
Alginate and methacrylated gelatin scaffolds	Extrusion	hUVECs	Cardiac	[210]
Nanofibrillated cellulose and alginate scaffolds	Extrusion	Chondrocytes	Cartilage	[50]
Methacrylated hyaluronan and methacrylated gelatin scaffolds	Extrusion	hAVIC	Cardiac	[211]
Thiol hyaluronic acid, thiol gelatin, dECM, and PEG-based crosslinkers in scaffolds	Extrusion	Multicellular primary cell liver spheroids	Liver	[212]
Gelatin, alginate, EGF, and dermal homogenates scaffolds	Extrusion	Epithelial progenitor cells	Sweat gland	[213]
Alginate, gellan and BioCartilage (micronized human cartilage particles) scaffolds	Co-extrusion	Chondrocytes	Cartilage	[214]
Cell-laden collagen core and alginate sheet scaffolds	Extrusion	hASCs	Liver	[215]
Heparin sulphate – laminine mimetic peptide amphiphile nanofibre scaffold	Freeze-drying	SH-SY5Y	Neurons	[216]
Nanofibrous PET scaffolds coated with collagen	Electrospinning	Caco-2 (human epithelial cells)	Intestinal epithelium	[217]
Polypyrrole-coated paclitaxel-loaded PCL fibrous scaffold	Electrospinning and membrane surface functionalization	–	Site-specific drug delivery platform with NIR (near-infrared) and pH-triggering for synergetic photothermal chemotherapy	[218]
PCL-collagen radially aligned nanofibre scaffolds	Modified electrospinning	rCCs (Rabbit corneal cells)	Cadaveric corneas and amniotic membranes	[219]
Fibroblast loaded collagen-based construct with PCL mesh	Hybrid extrusion and inkjet process	Keratinocytes	Human skin	[220]
TFG-β1 or gentamicin loaded PCL/collagen nanofibres	Electrospinning	Human dermal fibroblasts	Wound healing	[221]
Devitalized native cartilage with porous PCL scaffolds	Electrospinning	ASCs	Cartilage	[222]
Plasma-treated PLLA: PCL (4:1) nanofibrous scaffolds coated with Matrigel	Electrospinning	hESCs	Auditory nerve	[223]
PLLA, agar, and gelatin scaffolds	Thermally-induced phase separation	Chondrocytes	Cartilage	[224]
PLLA- fibronectin mimetic peptide fibrous scaffolds	Electrospinning	Human adult renal stem cells	Renal tubular epithelial lineage	[225]

bring different biomimetic architectures. There are three main approaches for developing cell-laden scaffolds (Fig. 6):

a) *scaffold-based* – this top-down strategy uses bioactive scaffolds acting like mechanical support for immobilization of cells and bioactive molecules; although applying good control over the scaffold characteristics (shape and size, biofunctionalization), usually, the initial cell density, tissue assembly and vascularization are poor;

b) *scaffold-free* - bottom-up approach where cell aggregates, sheets or spheroids are used as building blocks of the scaffolds; however, low biomolecule-functionalization ability and insufficient mechanical stability are the main disadvantages of this strategy;

c) *synergetic or bioassembly* – it uses bottom-up random assembly of multiple functional units (cell-laden modules) and combines the advantages of both previous strategies.

Such cell-containing microunits well replicate the physiological conditions (with efficient nutrient and oxygen transfer), possess high surface-to-volume ratio and can be arranged in the desired geometry. Nevertheless, this approach suffers from an inability to fabricate complex scaffolds with controlled micrometre-scaled features and when heterogeneous cell populations are assembled, poor functionality could occur [234].

As opposed to bioassembly, bioprinting bottom-up technologies use smaller fabrication units such as cells, cell aggregates or biochemicals to form scaffolds with ordinate assembly. The cells or bioactive moieties are included in bioinks of hydrogel precursors or ECM-containing solutions that are printed continuously or in the form of small droplets. The bioprinting technologies include extrusion-based [235], droplet-based ejection [236], laser-assisted [237], and hybrid methodologies. Extrusion-based bioprinters use either continuous cell-laden hydrogel (from chitosan, gelatin, fibrinogen, etc.) filaments or cell spheroids [238] that could be deposited without a scaffold. When a microtissue-based approach is used, smaller 3D spheroid aggregates in degradable carrying medium with uniform size and shape are incorporated into bioink that after printing consolidates into macrotissue [239]. This technique was successfully used for producing of simple tissues such as adipose tissue [240], muscles, bones, cartilage [241], 3D vasculature [235], neural mini-tissues differentiated to functional neurons and supporting neuroglia [242], and vascularized heart tissue [243]. Extrusion based printers are suitable for the production of large and complex (branched or tubular) structures but can be deficient for printing high-resolution or multiple cell-type structures. The droplet-based bioprinters dispense cell-loaded droplets from a nozzle by sonic, pneumatic or thermal actuation [244]. In valve-based droplet ejection, the size and number of cells in a droplet can be controlled by valve opening time or actuation frequency while in acoustic-based, picoliter cell-encapsulating droplet is generated with a few microseconds pulse duration. The droplet-based method proposes high-resolution, automation, versatility, and cell viability for the account of clogging and lower cell density [245]. Bone, cartilage tissue scaffolds [208], microvasculature constructions [246], and cardiac patch [247] have been fabricated by this method. Laser-assisted bioprinting (LAB) uses laser irradiation to assemble cell-containing microdroplets ejected from a ribbon on a substrate producing 2D and sometimes 3D architectures [248]. Although Koch et al. reported no or below detection deleterious effect of LAB on printed cells [249], there is a need for evaluation cell function and damage during and after printing in various hydrogels, temperature and rheological ranges compatible with bioprinting technologies.

Despite the recent developments of bioprinting, it is still a challenge to build high-resolution constructs from multiple cell-types patterned necessary for cell-cell interaction and function. One option is to print spatially defined gradients of immobilized GFs (at pico- to nanogram quantities) that influence the differentiation of seeded multi-potential cells such as neural stem cells [250] or mesenchymal stem cells [251].

It was reported that GF gradients could effectively direct individual cell migration and control cell alignment [108]. To fabricate complex cytoarchitectures, Graham et al. printed patterned construct of two populations of cells with high-resolution 3D features including layers and channels under 200 μm width within cubic mm-scaled structure [252]. They used dispensing nozzle ejecting cell-containing hydrogel-based bioink where the cellular constructs were encapsulated in a thin gel layer and printed in an oil phase. The obtained relevant tissue density was 3×10^7 cell mL^{-1}. The lamellar constructs of both cell types, human embryonic kidney cell (hEKC) derivate and ovine mesenchymal stem cell (oMSCs) in homogeneous distribution remained viable and responsive to growth factors for osteoblasts and chondrocytes differentiation.

For the successful implantation of the biomaterial, biomimetic structure seeded with cells either donated from the host or from compatible tissue bank is required. Even decellularized ECM (dECM) was found to be tissue-specific providing crucial cues for cell survival and function. Consequently, dECM bioinks from adipose (adECM) and cartilage (cdECM) tissue with encapsulated cells were used for the production of 3D porous scaffolds of dECM and PCL framework by multi-head tissue/organ building system [240]. The cell viability of the printed construct was over 95%. Using encapsulated human adipose-
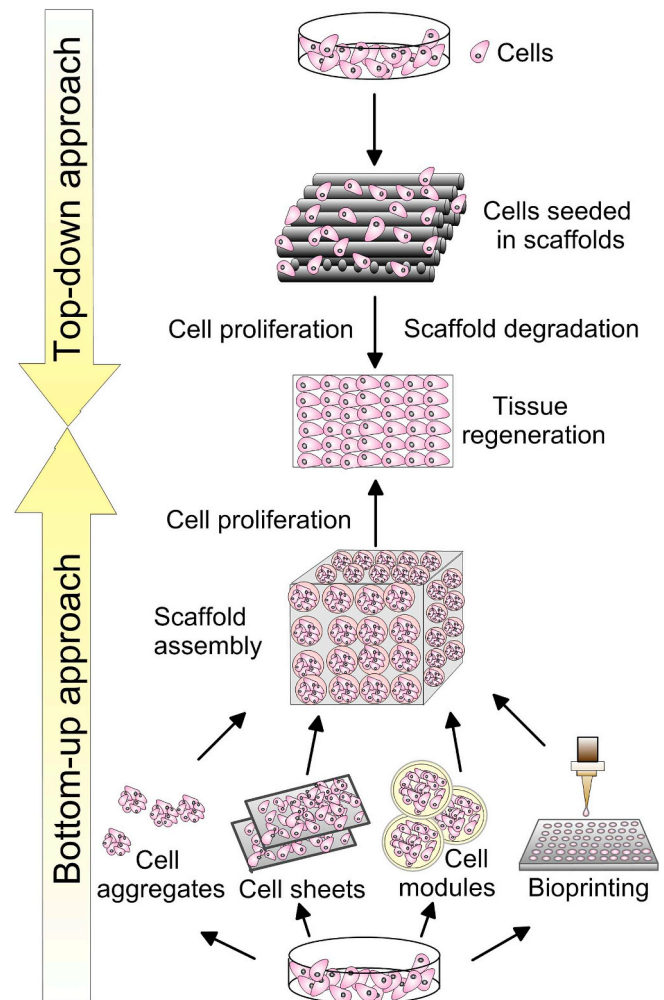
Fig. 6. Strategies for tissue regeneration by using cell-laden scaffolds: The top-down approach uses scaffolds biofunctionalized with cells and other biomolecules. The tissue is regenerated after cell proliferation and scaffold degradation. The bottom-up approach involves cell aggregates, sheets, modules or bioprinted elements to produce blocks for assembling the scaffolds needed for tissue regeneration.

derived stem cells (hADSCs) and human inferior turbinate-tissue derived mesenchymal stromal cells (hTMSCs) in adECM and cdECM, respectively, the authors generated a synergetic effect of combining engineered porosity with an increased commitment of stem cells towards specific differentiation [240].

Although expecting lower liver-specific functions, Cheng et al. [253] synthesized core-shell microgel scaffolds containing fibroblast loaded alginate shell and hepatocyte-filled aqueous core. In contrast to monotypic (without fibroblasts) counterpart, the co-cultured spheroids demonstrated increased urea synthesis and albumin secretion that are biomarkers used when the liver is drug-screened. The same research group was able to co-encapsulate hepatocytes and endothelial progenitor cells (EPCs) into alginate-collagen microgels that showed enhanced hepatocellular functions only at co-culture ratio 5:1, respectively [254]. The increase in EPCs fraction reduced the performance of hepatocytes. Moreover, it was hard to supply sufficient growth factors to the encapsulated in hydrogel cells for their differentiation.

In another study, Min et al. printed complex full-thickness skin construct containing pigmentation [255]. For that purpose, the scaffold consisted of five layers of collagen-precursor solution bioprinted in small cell-containing droplets and crosslinked through neutralization with $NaHCO_3$. A suspension of fibroblasts was embedded in 2–4 layers. On the top of the dermal layer, suspension of melanocytes was printed, followed by primary keratinocyte layers above it. When submerged in air-liquid interface (ALI) culture, the formation of distinct dermal and epidermal layers with terminal differentiation of keratinocytes was observed. The melanocytes and keratinocytes in the epidermal layer formed dark-pigmented non-uniform clusters underlining the need for optimization the pigmentation homogeneity.

It follows that high resolution, high-speed organization and high cell viability are key requirements for cell-laden 3D scaffold fabrication. After that, efficient vascularization precisely placed at a high level of density cells is an important precondition for successful implantation. Recently, using multiple bioinks loaded with vein endothelial cells, mesenchymal stem cells, and dermal fibroblasts for the synthesis of ECM, Kolesky et al. [209] bioprinted 3D vascularized tissue with thickness over 1 cm that actively perfused GFs to differentiate hMSCs towards osteogenesis. The 3D constructs underwent fast tissue maturation where the scaffold provided controllable growth, maturation, and proper differentiation. Similarly, Mori et al. printed skin equivalent containing perfusable vascular channels coated with endothelial cells [256]. The vascular channels with conventional epidermal and dermal morphology were opened in the perfused skin-equivalent because of the pressure generated by perfusion. The results confirmed the barrier function of the epidermal layer that could be controlled by changing the concentration of normal human epidermal keratinocytes (NHEKs). The vascular channel permeability was size-selective and controlled by VEGF. These successive constructions of vascular channels could make the implementation of sweat glands, hair, nervous and immune system components possible. However, still pending problems are the poor mechanical properties and limited biological interactions of hydrogels that could be effectively replaced by alternative types of bioinks such as supramolecular hydrogels that propose an easy modification, self-assembly properties, and tunable bioactive behaviour [257].

8. Challenges and future perspectives of biomaterials for 3D scaffolds

In this review, remarkable achievements in regenerative medicine and tissue engineering have been summarized. Advanced 3D scaffolds should not only provide support for regenerating tissue and transplanted cells but also achieve local release of regulatory or therapeutic substances. Such scaffolds that are able to satisfy various biochemical and/or functional requirements are usually produced by different combinations of biomaterials with specific complementary properties assisting local regeneration. The engineered constructs have benefitted

the biological effects of the complex scaffolds usually at the expense of applying complex engineered technologies. The advanced composite scaffolds could also segregate in two or more layers with smooth discrete gradients in chemical or physical properties that are able to organize and guide, and maintain multiple cellular phenotype structures and heterogeneous extracellular matrix morphogenesis.

Although considerable progress has been made in 3D scaffold research, many challenged have to be resolved that make the choice of a suitable scaffold and biomaterial quite difficult. It should be taken into account that cell- and growth factor-incorporated scaffolds are difficult to be stored because of their low viability and stability. Moreover, the long term release of immobilized substances does not always lead to achieving the desired effects in the microenvironment promoting functional recovery or providing trophic or anti-inflammatory support. Some of the major challenges of 3D scaffold involve:

a. Tuning the structural, biomechanical properties, and degradation rate of scaffolds with optimized surface characteristics to enhance cell contacts and ECM deposition depending on the intended application;
b. Efforts in combining different biomaterials with incorporated bioactive molecules and different fabrication methods for producing superior scaffolds for a specific application without burst release and easy inactivation;
c. Increased neurovascularization that inhibits localized necrosis and implant failure;
d. Formation of multi-tissue types scaffolds capable of spatial and functional cell regulation;
e. Increased resolution and accuracy of scaffold producing technologies enabling precise replication of fine tissue composition;
f. Minimizing the adverse effects and secondary damages;
g. Simplifying the process of fabrication;
h. Mass production outside the laboratory environment.

Resolving these issues, the 3D scaffold development may lead to improved tissue regeneration and move the application of 3D scaffold from screening purpose and evaluation in animals to intended clinical use. There is still a combination of factors including space constraint, biomechanical comparability, and other ultimately effecting changes in cell microenvironment predisposing cells toward attachment and influencing the regeneration process that is presently unknown.

Declaration of competing interest

None.

References

[1] H.N. Chia, B.M. Wu, Recent advances in 3D printing of biomaterials, J. Biol. Eng. 9 (2015) 4, https://doi.org/10.1186/s13036-015-0001-4.
[2] U. Jammalamadaka, K. Tappa, Recent advances in biomaterials for 3D printing and tissue engineering, J. Funct. Biomater. 9 (1) (2018) 22, https://doi.org/10.3390/jfb9010022.
[3] A.J. Engler, S. Sen, H.L. Sweeney, D.E. Discher, Matrix elasticity directs stem cell lineage specification, Cell 126 (2006) 677–689, https://doi.org/10.1016/j.cell.2006.06.044.
[4] E. Saiz, E.A. Zimmermann, J.S. Lee, U.G. Wegst, A.P. Tomsia, Perspectives on the role of nanotechnology in bone tissue engineering, Dent. Mater. 29 (2013) 103–115, https://doi.org/10.1016/j.dental.2012.08.001.
[5] L. Feng, E. Lingling, H. Liu, The effects of separating inferior alveolar neurovascular bundles on osteogenesis of tissue-engineered bone and vascularization, Biomed. Pap. Med. Fac. Univ. Palacky Olomouc Czech Repub. 159 (4) (2015) 637–641, https://doi.org/10.5507/bp.2014.050.

[6] A. Marrella, T.Y. Lee, D.H. Lee, S. Karuthedom, D. Syla, A. Chawla, A. Khademhosseini, H.L. Jang, Engineering vascularized and innervated bone biomaterials for improved skeletal tissue regeneration, Mater. Today 21 (4) (2018) 362–376, https://doi.org/10.1016/j.mattod.2017.10.005.

[7] S. Shruti, A.J. Salinas, G. Lusvardi, G. Malavasi, L. Menabue, M. Vallet-Regi, Mesoporous bioactive scaffolds prepared with cerium-, gallium- and zinc-containing glasses, Acta Biomater. 9 (1) (2013) 4836–4844, https://doi.org/10.1016/j.actbio.2012.09.024.

[8] G. Wei, P.X. Ma, Structure and properties of nano-hydroxyapatite/polymer composite scaffolds for bone tissue engineering, Biomaterials 25 (19) (2004) 4749–4757, https://doi.org/10.1016/j.biomaterials.2003.12.005.

[9] B.D. Boyan, T.W. Hummert, D.D. Dean, Z. Schwartz, Role of material surfaces in regulating bone and cartilage cell response, Biomaterials 17 (2) (1996) 137–146, https://doi.org/10.1016/0142-9612(96)85758-9.

[10] M. Lee, B.M. Wu, J.C. Dunn, Effect of scaffold architecture and pore size on smooth muscle cell growth, J. Biomed. Mater. Res. A 87 (4) (2008) 1010–1016, https://doi.org/10.1002/jbm.a.31816.

[11] S.F. Hulbert, F.A. Young, R.S. Mathews, J.J. Klawitter, C.D. Talbert, F.H. Stelling, Potential of ceramic materials as permanently implantable skeletal prostheses, J. Biomed. Mater. Res. 4 (3) (1970) 433–456, https://doi.org/10.1002/jbm.820040309.

[12] V. Mouriño, A.R. Boccaccini, Bone tissue engineering therapeutics: controlled drug delivery in three-dimensional scaffolds, J. R. Soc. Interface 7 (2012) 209–227, https://doi.org/10.1098/rsif.2009.0379.

[13] S.A. Bencherif, T.M. Braschler, P. Renaud, Advances in the design of macroporous polymer scaffolds for potential applications in dentistry, J. Periodontal Implant Sci. 43 (2013) 251–261, https://doi.org/10.5051/jpis.2013.43.6.251.

[14] M. Rampichová, M. Buzgo, J. Chvojka, E. Prosecká, O. Kofroňová, E. Amler, Cell penetration to nanofibrous scaffolds, Cell Adhes. Migrat. 8 (2014) 36–41, https://doi.org/10.4161/cam.27477.

[15] L. Ren, V. Pandit, J. Elkin, T. Denman, J.A. Cooper, S.P. Kotha, Large-scale and highly efficient synthesis of micro- and nano-fibres with controlled fiber morphology by centrifugal jet spinning for tissue regeneration, Nanoscale 5 (2013) 2337–2345, https://doi.org/10.1039/C3NR33423F.

[16] L. Wang, J. Shi, L. Liu, E. Secret, Y. Chen, Fabrication of polymer fiber scaffolds by centrifugal spinning for cell culture studies, Microelectron. Eng. 88 (2011) 1718–1721, https://doi.org/10.1016/j.mee.2010.12.054.

[17] A. Loordhuswamy, V. Krishnaswamy, P. Korrapati, S. Thinakaran, G. Rengaswami, Fabrication of highly aligned fibrous scaffolds for tissue regeneration by centrifugal spinning technology, Mater. Sci. Eng. C 42 (2014) 799–807, https://doi.org/10.1016/j.msec.2014.06.011.

[18] F. Xu, B. Weng, A.M. Luis, A. Kuang, A.T. Jorge, K. Lozano, Fabrication of cellulose fine fibre-based membranes embedded with silver nanoparticles via Forcespinning, J. Polym. Eng. 36 (2016) 269–278, https://doi.org/10.1515/polyeng-2015-0092.

[19] J. Melke, S. Midha, S. Ghosh, K. Ito, S. Hofmann, Silk fibroin as a biomaterial for bone tissue engineering, Acta Biomater. 31 (2016) 1–16, https://doi.org/10.1016/j.actbio.2015.09.005.

[20] R. Vasita, D.S. Katti, Nanofibers and their applications in tissue engineering, Int. J. Nanomed. 1 (1) (2006) 15–30. PMC2426767.

[21] H. Xia, Q. Chen, Y. Fang, D. Liu, D. Zhong, H. Wu, Y. Xia, Y. Yan, W. Tang, X. Sun, Directed neurite growth of rat dorsal root ganglion neurons and increased colocalization with Schwann cells on aligned poly(methyl methacrylate) electrospun nanofibers, Brain Res. Elsevier 1565 (2014) 18–27, https://doi.org/10.1016/j.brainres.2014.04.002.

[22] L.B. Hejazian, B. Esmaeilzade, F.M. Ghoroghi, F. Moradi, M.B. Hejazian, A. Aslani, The role of biodegradable engineered nanofiber scaffolds seeded with hair follicle stem cells for tissue engineering, Iran, Biomed. J. 16 (2012) 193–201, https://doi.org/10.6091/ibj.1074.2012.

[23] R.J. WadeabJason, A. Burdick, Advances in nanofibrous scaffolds for biomedical applications: from electrospinning to self-assembly, Nano Today 9 (6) (2014) 722–742, https://doi.org/10.1016/j.nantod.2014.10.002.

[24] G.T. Christopherson, H. Song, H.-Q. Mao, The influence of fibre diameter of electrospun substrates on neural stem cell differentiation and proliferation, Biomaterials 30 (2009) 556–564, https://doi.org/10.1016/j.biomaterials.2008.10.004.

[25] A. Repanas, S. Andriopoulou, B. Glasmacher, The significance of electrospinning as a method to create fibrous scaffolds for biomedical engineering and drug delivery applications, J. Drug Deliv. Sci. Technol. 31 (2016) 137–146, https://doi.org/10.1016/j.jddst.2015.12.007.

[26] Q. Yao, J.G.L. Cosme, T. Xu, J.M. Miszuk, P.H.S. Picciani, H. Fong, H. Sun, Three dimensional electrospun PCL/PLA blend nanofibrous scaffolds with significantly improved stem cells osteogenic differentiation and cranial bone formation, Biomaterials 115 (2017) 115–127, https://doi.org/10.1016/j.biomaterials.2016.11.018.

[27] J.M. Corey, D.Y. Lin, K.B. Mycek, Q. Chen, S. Samuel, E.L. Feldman, Aligned electrospun nanofibers specify the direction of dorsal root ganglia neurite growth, J. Biomed. Mater. Res. A 83A (2007) 636–645, https://doi.org/10.1002/jbm.a.31285.

[28] M.E. Frohbergh, A. Katsman, G.P. Botta, P. Lazarovici, C.L. Schauer, U.G. Wegst, Electrospun hydroxyapatite-containing chitosan nanofibers crosslinked with genipin for bone tissue engineering, Biomaterials 33 (2012) 9167–9178, https://doi.org/10.1016/j.biomaterials.2012.09.009.

[29] Z. Yin, X. Chen, H.X. Song, J.-j. Hu, Q.-m. Tang, T. Zhu, W.-l. Shen, J.-l. Chen, H. Liu, B.C. Heng, H.-W. Ouyang, Electrospun scaffolds for multiple tissues regeneration in vivo through topography dependent induction of lineage-specific differentiation, Biomaterials 44 (2015) 173–185, https://doi.org/10.1016/j.biomaterials.2014.12.027.

[30] J. Cai, J. Wang, K. Ye, D. Li, C. Ai, D. Sheng, W. Jin, X. Liu, Y. Zhi, J. Jiang, J. Chen, X. Mo, S. Chen, Dual-layer aligned-random nanofibrous scaffolds for improving gradient microstructure of tendon-to the -bone healing in a rabbit extra-articular model, Int. J. Nanomed. 13 (2018) 3481–3492, https://doi.org/10.2147/IJN.S165633.

[31] T. Subbiah, G. Bhat, R. Tock, S. Parameswaran, S. Ramkumar, Electrospinning of nanofibers, J. Appl. Polym. Sci. 96 (2005) 557–569, https://doi.org/10.1002/app.21481.

[32] D. Stephens, L. Li, D. Robinson, S. Chen, H. Chang, R.M. Liu, Y. Tian, E.J. Ginsburg, X. Gao, T. Stultz, Investigation of the in vitro release of gentamicin from a polyanhydride matrix, J. Control. Release 63 (3) (2000) 305–317, https://doi.org/10.1016/S0168-3659(99)00205-9.

[33] L. Brannon-Peppas, Recent advances in the use of biodegradable microparticles and nanoparticles in controlled drug delivery, Int. J. Pharm. 116 (1995) 1–9, https://doi.org/10.1016/0378-5173(94)00324-X.

[34] N.M. Bergmann, N.A. Peppas, Molecularly imprinted polymers with specific recognition for macromolecules and proteins, Prog. Polym. Sci. 33 (2008) 271–288, https://doi.org/10.1016/j.progpolymsci.2007.09.004.

[35] H.B. Ravivarapu, K. Burton, P.P. DeLuca, Polymer and microsphere blending to alter the release of a peptide from PLGA microspheres, Eur. J. Pharm. Biopharm. 50 (2) (2000) 263–270, https://doi.org/10.1016/S0939-6411(00)00099-0.

[36] Y. Hu, J. Hollinger, K. Marra, Controlled release from coated polymer microparticles embedded in tissue-engineered scaffolds, J. Drug Target. 9 (2001) 431–438, https://doi.org/10.3109/10611860108998777.

[37] B. Dhandayuthapani, Y. Yoshida, T. Maekawa, D.S. Kumar, Polymeric scaffolds in tissue engineering application: a review, Int. J. Polymer Sci. Art. ID 290602 (2011) 1–19, https://doi.org/10.1155/2011/290602.

[38] M. Borden, M. Attawia, C.T. Laurencin, The sintered microsphere matrix for bone tissue engineering: in vitro osteoconductivity studies, J. Biomed. Mater. Res. 61 (3) (2002) 421–429, https://doi.org/10.1002/jbm.10201.

[39] T. Yoshii, A.E. Hafeman, J.M. Esparza, A. Okawa, S.A. Guelcher, Local injection of lovastatin in biodegradable polyurethane scaffolds enhances bone regeneration in a critical-sized segmental defect in rat femora, J. Tissue Eng. Regenerat. Med. 8 (2014) 589–595, https://doi.org/10.1002/term.1547.

[40] M. Radisic, L. Yang, J. Boublik, R.J. Cohen, R. Langer, L.E. Freed, G. Vunjak-Novakovic, Medium perfusion enables engineering of compact and contractile cardiac tissue, Am. J. Physiol. Heart Circ. Physiol. 286 (2) (2004) H507–H516, https://doi.org/10.1152/ajpheart.00171.2003.

[41] W. Fan, R. Crawford, Y. Xiao, Enhancing in vivo vascularized bone formation by cobalt chloride-treated bone marrow stromal cells in a tissue-engineered periosteum model, Biomaterials 31 (13) (2010) 3580–3589, https://doi.org/10.1016/j.biomaterials.2010.01.083.

[42] D.H. Kempen, L. Lu, A. Heijink, T.E. Hefferan, L.B. Creemers, A. Maran, Effect of local sequential VEGF and BMP-2 delivery on ectopic and orthotopic bone regeneration, Biomaterials 30 (2009) 2816–2825, https://doi.org/10.1016/j.biomaterials.2009.01.031.

[43] G. Turnbull, J. Clarke, F. Picard, P. Riches, L. Jia, F. Han, B. Li, W. Shu, 3D bioactive composite scaffolds for bone tissue engineering, Bioact. Mater. 3 (2018) 278–314, https://doi.org/10.1016/j.bioactmat.2017.10.001.

[44] L. Shor, S. Güçeri, X. Wen, M. Gandhi, W. Sun, Fabrication of three-dimensional polycaprolactone/hydroxyapatite tissue scaffolds and osteoblast-scaffold interactions in vitro, Biomaterials 28 (35) (2007) 5291–5297, https://doi.org/10.1016/j.biomaterials.2007.08.018.

[45] C. Deng, J. Chang, C. Wu, Bioactive scaffolds for osteochondral regeneration, J. Orthop. Transl. 17 (2019) 15–25, https://doi.org/10.1016/j.jot.2018.11.006.

[46] P. Datta, A. Dhawan, Y. Yu, D. Hayes, H. Gudapati, I.T. Ozbolat, Bioprinting of osteochondral tissues: a perspective on current gaps and future trends, Int. J. Bioprint. 3 (2) (2017) 109–120, https://doi.org/10.18063/IJB.2017.02.007.

[47] J.K. Algardh, T. Horn, H. West, R. Aman, A. Snis, H. Engqvist, J. Lausmaa, O. Harrysson, Thickness dependency of mechanical properties from thin-walled titanium parts manufactured by electron beam melting (EBM), Add, Man (Lond.) 12 (2016) 45–50, https://doi.org/10.1016/j.addma.2016.06.009.

[48] Y. Yang, G. Wang, H. Liang, C. Gao, S. Peng, L. Shen, C. Shuai, Additive manufacturing of bone scaffolds, Int. J. Bioprint. 5 (1) (2019) 148–173, https://doi.org/10.18063/IJB.v5i1.148.

[49] S.V. Murphy, A. Atala, 3D bioprinting of tissues and organs, Nat. Biotechnol. 32 (2014) 773–785, https://doi.org/10.1038/nbt.2958.

[50] K. Markstedt, A. Mantas, I. Tournier, H. Martínez Ávila, D. Hägg, P. Gatenholm, 3D bioprinting human chondrocytes with nanocellulose–alginate bioink for cartilage tissue engineering applications, Biomacromolecules 16 (2015) 1489–1496, https://doi.org/10.1021/acs.biomac.5b00188.

[51] Y. Zhang, C. Wang, L. Fu, S. Ye, M. Wang, Y. Zhou, Fabrication and application of novel porous scaffold in situ-loaded graphene oxide and osteogenic peptide by cryogenic 3D printing for repairing critical-sized bone defect, Molecules 24 (2019) 1669, https://doi.org/10.3390/molecules24091669.

[52] D. Gorth, T. J Webster, Matrices for Tissue Engineering and Regenerative Medicine, Biomaterials for Artificial Organs, Woodhead Publishing Series in Biomaterials, 2011, pp. 270–286, https://doi.org/10.1533/9780857090843.2.270.

[53] A.S. Hoffman, Hydrogels for biomedical applications, Adv. Drug Deliv. Rev. 64 (2012) 18–23, https://doi.org/10.1016/S0169-409X(01)00239-3.

[54] I.M. El-Sherbiny, M.H. Yacoub, Hydrogel scaffolds for tissue engineering, progress and challenges, Global Cardiol. Sci. Practice 38 (2013) 1–27, https://doi.org/10.5339/gcsp.2013.38.

[55] R.H. Schmedlen, K.S. Masters, J.L. West, Photocrosslinkable polyvinyl alcohol hydrogels that can be modified with cell adhesion peptides for use in tissue engineering, Biomaterials 23 (2002) 4325–4332, https://doi.org/10.1016/s0142-9612(02)00177-1.

[56] E. Guadalupe, D. Ramos, N.B. Shelke, R. James, C. Gibney, S.G. Kumbar, Bioactive polymeric nanofiber matrices for skin regeneration, J. Appl. Polym. Sci. 132 (2015) 41879–41889, https://doi.org/10.1002/app.41879.

[57] I. Aizman, C.C. Tate, M. McGrogan, C.C. Case, Extracellular matrix produced by bone marrow stromal cells and by their derivative, SB623 cells, supports neural cell growth, J. Neurosci. Res. 87 (2009) 3198–3206, https://doi.org/10.1002/jnr.22146.

[58] S. Zia, M. Mozafari, G. Natasha, A. Tan, Z. Cui, A.M. Seifalian, Hearts beating through decellularized scaffolds: whole-organ engineering for cardiac regeneration and transplantation, Crit. Rev. Biotechnol. 36 (2016) 705–715, https://doi.org/10.3109/07388551.2015.1007495.

[59] A. Crabbé, Y. Liu, S.F. Sarker, N.R. Bonenfant, J. Barrila, Z.D. Borg, Recellularization of Decellularized Lung Scaffolds Is Enhanced by Dynamic Suspension Culture vol. 10, (2015) e0126846, , https://doi.org/10.1371/journal.pone.0126846.

[60] F. Chen, J.J. Yoo, A. Atala, Acellular collagen matrix as a possible 'off the shelf' biomaterial for urethral repair, Urology 54 (3) (1999) 407–410, https://doi.org/10.1016/s0090-4295(99)00179-x.

[61] H. Rasti, N. Saghiri, J. Baharara, N. Mahdavi-Shahri, M. Marjani, S.H. Alavi, Differentiation of blastema cells in decellularized bladder scaffold in vitro, Zahedan J. Res. Med. Sci. 17 (5) (2015) e960, , https://doi.org/10.17795/zjrms960.

[62] D. Rana, H. Zreiqat, N. Benkirane-Jessel, S. Ramakrishna, M. Ramalingam, Development of decellularized scaffolds for stem cell-driven tissue engineering, J. Tissue Eng. Regenerat. Med. 11 (4) (2015) 942–965, https://doi.org/10.1002/term.2061.

[63] Y. Lai, Y. Sun, C.M. Skinner, E.L. Son, Z. Lu, R.S. Tuan, R.L. Jilka, J. Ling, X.-D. Chen, Reconstitution of marrow-derived extracellular matrix ex vivo: a robust culture system for expanding large-scale highly functional human mesenchymal stem cells, Stem Cells Dev. 19 (2010) 1095–1107, https://doi.org/10.1089/scd.2009.0217.

[64] B. Chan, K. Leong, Scaffolding in tissue engineering: general approaches and tissue-specific considerations, Eur. Spine J. 17 (2008) 467–479, https://doi.org/10.1007/s00586-008-0745-3.

[65] L. Hang, G. Yang, T. Jian, R.S. Tuan, Influence of decellularized matrix derived from human mesenchymal stem cells on their proliferation, migration and multi-lineage differentiation potential, Biomaterials 33 (18) (2012) 4480–4489, https://doi.org/10.1016/j.biomaterials.2012.03.012.

[66] A. Evangelatov, R. Pankov, The evolution of three-dimensional cell cultures towards unimpeded regenerative medicine and tissue engineering, in: J.A. Andrades (Ed.), Regen. Med. Tissue Eng. 2013 IntechOpen https://www.intechopen.com/books/regenerative-medicine-and-tissue-engineering/the-evolution-of-three-dimensional-cell-cultures-towards-unimpeded-regenerative-medicine-and-tissue-.

[67] S. Pacelli, S. Basu, J. Whitlow, A. Chakravarti, F. Acosta, A. Varshney, S. Modaresi, C. Berkland, A. Paul, Strategies to develop endogenous stem cell-recruiting bioactive materials for tissue repair and regeneration, Adv. Drug Deliv. Rev. 120 (2017) 50–70, https://doi.org/10.1016/j.addr.2017.07.011.

[68] J. Li, K.C. Hansen, Y. Zhang, C. Dong, C.Z. Dinu, M. Dzieciatkowska, M. Pei, Rejuvenation of chondrogenic potential in a young stem cell microenvironment, Biomaterials 35 (2) (2014) 642–653, https://doi.org/10.1016/j.biomaterials.2013.09.099.

[69] P. Chocholata, V. Kulda, V. Babuska, Fabrication of scaffolds for bone-tissue regeneration, Materials 12 (2019) 568, https://doi.org/10.3390/ma12040568.

[70] D. Yoo, New paradigms in hierarchical porous scaffold design for tissue engineering, Mater. Sci. Eng. C 33 (2013) 1759–1772, https://doi.org/10.1016/j.msec.2012.12.092.

[71] F. Yang, C. Chen, Q. Zhou, Y. Gong, R. Li, C. Li, F. Klämpfl, S. Freund, X. Wu, Y. Sun, X. Li, M. Schmidt, D. Ma, Y.C. Yu, Laser beam melting 3D printing of Ti6Al4V based porous structured dental implants: fabrication, biocompatibility analysis and photoelastic study, Sci. Rep. 7 (2017) 45360, https://doi.org/10.1038/srep45360.

[72] B. Zhao, H. Wang, N. Qiao, C. Wang, M. Hu, Corrosion resistance characteristics of a Ti–6Al–4V alloy scaffold that is fabricated by electron beam melting and selective laser melting for implantation in vivo, Mater. Sci. Eng. C 70 (2016) 832–841, https://doi.org/10.1016/j.msec.2016.07.045.

[73] M.A. Surmeneva, R.A. Surmenev, E.A. Chudinova, A. Koptioug, M.S. Tkachev, S.N. Gorodzha, L.-E. Rännar, Fabrication of multiple-layered gradient cellular metal scaffold via electron beam melting for segmental bone reconstruction, Mater. Des. 133 (2017) 195–204, https://doi.org/10.1016/j.matdes.2017.07.059.

[74] F.A. Shah, O. Omar, F. Suska, A. Snis, A. Matic, L. Emanuelsson, B. Norlindh, J. Lausmaa, P. Thomsen, A. Palmquist, Long–term osseointegration of 3D printed CoCr constructs with an interconnected open-pore architecture prepared by electron beam melting, Acta Biomater. 36 (2016) 296–309, https://doi.org/10.1016/j.actbio.2016.03.033.

[75] M. Fousová, J. Kubásek, D. Vojtěch, J. Fort, J. Čapek, 3D printed porous stainless steel for potential use in medicine, IOP Conf. Ser. Mater. Sci. Eng. 179 (2017) 012025, , https://doi.org/10.1088/1757-899X/179/1/012025.

[76] J. van den Dolder, E. Farber, P.H.M. Spauwen, J.A. Jansen, Bone tissue reconstruction using titanium fibre mesh combined with rat bone marrow stromal cells, Biomaterials 24 (10) (2003) 1745–1750, https://doi.org/10.1016/S0142-9612(02)00537-9.

[77] K. Bobe, E. Willbold, I. Morgenthal, O. Andersen, T. Studnitzky, J. Nellesen, W. Tillmann, C. Vogt, K. Vano, F. Witte, In vitro and in vivo evaluation of biodegradable, open-porous scaffolds made of sintered magnesium W4 short fibres, Acta Biomater. 9 (2013) 8611–8623, https://doi.org/10.1016/j.actbio.2013.03.035.

[78] F. Witte, H. Ulrich, M. Rudert, E. Willbold, Biodegradable magnesium scaffolds: Part 1: appropriate inflammatory response, J. Biomed. Mater. Res. A 81 (2007) 748–756, https://doi.org/10.1002/jbm.a.31170.

[79] M.-Q. Cheng, T. Wahafu, G.-F. Jiang, W. Liu, Y.-Q. Qiao, X.-C. Peng, T. Cheng, X.-L. Zhang, G. He, X.-Y. Liu, A novel open-porous magnesium scaffold with controllable microstructures and properties for bone regeneration, Sci. Rep. 6 (2016) 24134, https://doi.org/10.1038/srep24134.

[80] F. Witte, H. Ulrich, C. Palm, E. Willbold, Biodegradable magnesium scaffolds: Part II: peri-implant bone remodelling, J. Biomed. Mater. Res. A 81A (2007) 757–765, https://doi.org/10.1002/jbm.a.31293.

[81] P. Han, P. Cheng, S. Zhang, C. Zhao, J. Ni, Y. Zhang, W. Zhong, P. Hou, X. Zhang, Y. Zheng, Y. Chai, In vitro and in vivo studies on the degradation of high-purity Mg (99.99wt.%) screw with femoral intracondylar fractured rabbit model, Biomaterials 64 (2015) 57–69, https://doi.org/10.1016/j.biomaterials.2015.06.031.

[82] M.P. Staiger, A.M. Pietak, J. Huadmai, G. Dias, Magnesium and its alloys as orthopaedic biomaterials: a review, Biomaterials 27 (9) (2006) 1728–1734, https://doi.org/10.1016/j.biomaterials.2005.10.003.

[83] E. Zhang, D. Yin, L. Xu, L. Yang, K. Yang, Microstructure, mechanical and corrosion properties and biocompatibility of Mg–Zn–Mn alloys for biomedical application, Mater. Sci. Eng. C 29 (2009) 987–993, https://doi.org/10.1016/j.msec.2008.08.024.

[84] L.L. Hench, Bioceramics: from concept to clinic, J. Am. Ceram. Soc. 74 (1991) 1487–1510, https://doi.org/10.1111/j.1151-2916.1991.tb07132.x.

[85] V.S. Komlev, V.K. Popov, A.V. Mironov, A. Yu, Fedotov, A. Yu Teterina, I.V. Smirnov, I.Y. Bozo, V.A. Rybko, R.V. Deev, 3D printing of octacalcium phosphate bone substitutes, Front. Bioeng. Biotechnol. 3 (2015) 81, https://doi.org/10.3389/fbioe.2015.00081.

[86] C.F.L. Santos, A.P. Silva, L. Lopes, I. Pires, I.J. Correia, Design and production of sintered β-tricalcium phosphate 3D scaffolds for bone tissue regeneration, Mater. Sci. Eng. C 32 (5) (2012) 1293–1298, https://doi.org/10.1016/j.msec.2012.04.010.

[87] C. Deng, Q. Yao, C. Feng, J. Li, L. Wang, G. Cheng, M. Shi, L. Chen, J. Chang, C. Wu, 3D printing of bilineage constructive biomaterials for bone and cartilage regeneration, Adv. Funct. Mater. 27 (36) (2017) 1703117, https://doi.org/10.1002/adfm.201703117.

[88] G.A. Fielding, A. Bandyopadhyay, S. Bose, Effects of silica and zinc oxide doping on mechanical and biological properties of 3D printed tricalcium phosphate tissue engineering scaffolds, Dent. Mater. 28 (2) (2012) 113–122, https://doi.org/10.1016/j.dental.2011.09.010.

[89] A.M. Pietak, J.W. Reid, M.J. Stott, M. Sayer, Silicon substitution in the calcium phosphate bioceramics, Biomaterials 28 (2007) 4023–4032, https://doi.org/10.1016/j.biomaterials.2007.05.003.

[90] C.H. Chang, C.Y. Lin, F.H. Liu, M.H.C. Chen, C.P. Lin, H.N. Ho, Y.S. Liao, 3D printing bioceramic porous scaffolds with good mechanical property and cell affinity, PLoS One 10 (2015) e0143713, , https://doi.org/10.1371/journal.pone.0143713.

[91] X. Qi, P. Pei, M. Zhu, X. Du, C. Xin, S. Zhao, X. Li, Y. Zhu, Three-dimensional printing of calcium sulfate and mesoporous bioactive glass scaffolds for improving bone regeneration in vitro and in vivo, Sci. Rep. 7 (2017) 2–13, https://doi.org/10.1038/srep42556.

[92] C. Li, C. Jiang, Y. Deng, T. Li, N. Li, M. Peng, J. Wang, RhBMP-2 loaded 3D-printed mesoporous silica/calcium phosphate cement porous scaffolds with enhanced vascularization and osteogenesis properties, Sci. Rep. 7 (2017) 41331, https://doi.org/10.1038/srep41331.

[93] C. Wu, Y. Zhou, C. Lin, J. Chang, Y. Xiao, Strontium-containing mesoporous bioactive glass scaffolds with improved osteogenic/cementogenic differentiation of periodontal ligament cells for periodontal tissue engineering, Acta Biomater. 8 (2012) 3805–3815, https://doi.org/10.1016/j.actbio.2012.06.023.

[94] Y. Zhu, X. Li, J. Yang, S. Wang, H. Gao, N. Hanagata, Composition–structure-property relationships of the CaO–MxOy–SiO2–P2O5 (M = Zr, Mg, Sr) mesoporous bioactive glass (MBG) scaffolds, J. Mater. Chem. 21 (2011) 9208–9218, https://doi.org/10.1039/C1JM10838G.

[95] X. Wang, X. Li, A. Ito, Y. Sogo, Synthesis and characterization of hierarchically macroporous and mesoporous CaO–MO–SiO2–P2O5 (M = Mg, Zn, Sr) bioactive glass scaffolds, Acta Biomater. 7 (2011) 3638–3644, https://doi.org/10.1016/j.actbio.2011.06.029.

[96] Y. Zhu, Y. Zhang, C. Wu, Y. Fang, J. Yang, S. Wang, The effect of zirconium incorporation on the physicochemical and biological properties of mesoporous bioactive glass scaffolds, Microporous Mesoporous Mater. 143 (2011) 311–319, https://doi.org/10.1016/j.micromeso.2011.03.007.

[97] S.P. Valappil, D. Ready, E.A. Abou Neel, D.M. Pickup, L.A. Ó'Dell, W. Chrzanowski, J. Pratten, R.J. Newport, M.E. Smith, M. Wilson, J.C. Knowles, Controlled delivery of antimicrobial gallium ions from phosphate-based glasses, Acta Biomater. 5 (2009) 1198–1210, https://doi.org/10.1016/j.actbio.2008.09.019.

[98] C. Wu, R. Miron, A. Sculean, S. Kaskel, T. Doert, R. Schulze, Y. Zhang, Proliferation, differentiation and gene expression of osteoblasts in boron-containing associated with dexamethasone deliver from mesoporous bioactive glass scaffolds, Biomaterials 32 (29) (2011) 7068–7078, https://doi.org/10.1016/j.biomaterials.2011.06.009.

[99] C. Wu, W. Fan, Y. Zhu, M. Gelinsky, J. Chang, G. Cuniberti, V. Albrecht, T. Friis,

Y. Xiao, Multifunctional magnetic mesoporous bioactive glass scaffolds with a hierarchical pore structure, Acta Biomater. 7 (10) (2011) 3563–3572, https://doi.org/10.1016/j.actbio.2011.06.028.

[100] J. Zhang, S. Zhao, Y. Zhu, Y. Huang, M. Zhu, C. Tao, C. Zhang, Three-dimensional printing of strontium-containing mesoporous bioactive glass scaffolds for bone regeneration, Acta Biomater. 10 (5) (2014) 2269–2281, https://doi.org/10.1016/j.actbio.2014.01.001.

[101] C. Wu, Y. Zhou, M. Xu, P. Han, L. Chen, J. Chang, Y. Xiao, Copper-containing mesoporous bioactive glass scaffolds with multifunctional properties of angiogenesis capacity, osteostimulation and antibacterial activity, Biomaterials 34 (2013) 422–433, https://doi.org/10.1016/j.biomaterials.2012.09.066.

[102] T. Kokubo, H.M. Kim, M. Kawashita, Novel bioactive materials with different mechanical properties, Biomaterials 24 (13) (2003) 2161–2175, https://doi.org/10.1016/s0142-9612(03)00044-9.

[103] G.Y. Yang, J. Liu, F. Li, Z. Pan, X. Ni, Y. Shen, H. Xu, Q. Huang, Bioactive calcium sulfate/magnesium phosphate cement for bone substitute applications, Mater. Sci. Eng. C 35 (2014) 70–76, https://doi.org/10.1016/j.msec.2013.10.016.

[104] C.T. Wu, W. Fan, Y.H. Zhou, Y.X. Luo, M. Gelinsky, J. Chang, Y. Xiao, 3D-printing of highly uniform CaSiO3 ceramic scaffolds: preparation, characterization and in vivo osteogenesis, J. Mater. Chem. 22 (24) (2012) 12288–12295, https://doi.org/10.1039/C2JM30566F.

[105] V. Portici, J. Amendola, J. Laurin, D. Gigmes, L. Madaschi, S. Carelli, T. Marquette, A. Gorio, P. Decherchi, The use of poly(N-[2-hydroxypropyl]-methacrylamide) hydrogel to repair a T10 spinal cord hemisection in rat: a behavioural, electrophysiological and anatomical examination, ASN Neuro 5 (2) (2013) 149–166, https://doi.org/10.1042/AN20120082.

[106] T. Valdes-Sanchez, F.J. Rodriguez-Jimenez, D.M. Garcia-Cruz, J.L. Escobar-Ivirico, A. Alastrue-Agudo, S. Erceg, M. Monleon, V. Moreno-Manzano, Methacrylate-endcapped caprolactone and FM19G11 provide a proper niche for spinal cord-derived neural cells, J. Tissue Eng. Regenerat. Med. 9 (6) (2015) 734–739, https://doi.org/10.1002/term.1735.

[107] M. Xie, L. Wang, J. Ge, B. Guo, P.X. Ma, Strong electroactive biodegradable shape memory polymer networks based on star-shaped polylactide and aniline trimer for bone tissue engineering, ACS Appl. Mater. Interfaces 7 (12) (2015) 6772–6781, https://doi.org/10.1021/acsami.5b00191.

[108] W. Wang, K.W.K. Yeung, Bone grafts and biomaterials substitutes for bone defect repair: a review, Bioactive Materials 2 (4) (2017) 224–247, https://doi.org/10.1016/j.bioactmat.2017.05.007.

[109] C. Bertoldi, D. Zaffe, U. Consolo, Polylactide/polyglycolide copolymer in bone defect healing in humans, Biomaterials 29 (12) (2008) 1817–1823, https://doi.org/10.1016/j.biomaterials.2007.12.034.

[110] D.P. Bhattarai, L.E. Aguilar, C.H. Park, C.S. Kim, A review on properties of natural and synthetic based electrospun fibrous materials for bone tissue engineering, Membranes 8 (2018) 62, https://doi.org/10.3390/membranes8030062.

[111] D.B. Rifkin, R. Mazzieri, J.S. Munger, I. Noguera, J. Sung, Proteolytic control of growth factor availability, Apmis 107 (1999) 80–85, https://doi.org/10.1111/j.1699-0463.1999.tb01529.x.

[112] R. Reyes, A. Delgado, E. Sánchez, A. Fernández, A. Hernández, C. Evora, Repair of an osteochondral defect by sustained delivery of BMP-2 or TGFβ1 from a bilayered alginate-PLGA scaffold, J. Tissue Eng. Regen. Me ofd. 8 (7) (2012) 521–533, https://doi.org/10.1002/term.

[113] E.D.F. Ker, A.S. Nain, L.E. Weiss, J. Wang, J. Suhan, C.H. Amon, P.G. Campbell, Bioprinting of growth factors onto aligned sub-micron fibrous scaffolds for simultaneous control of cell differentiation and alignment, Biomaterials 32 (2011) 8097–8107, https://doi.org/10.1016/j.biomaterials.2011.07.025.

[114] H.W. Kim, E.J. Lee, I.K. Jun, H.E. Kim, J.C. Knowles, Degradation and drug release of phosphate glass/polycaprolactone biological composites for hard-tissue regeneration, J. Biomed. Mater. Res. B 75 (1) (2005) 34–41, https://doi.org/10.1002/jbm.b.30223.

[115] E.V. Melnik, S.N. Shkarina, S.I. Ivlev, V. Weinhardt, T. Baumbach, M.V. Chaikina, M.A. Surmeneva, R.A. Surmenev, In vitro degradation behaviour of hybrid electrospun scaffolds of polycaprolactone and strontium-containing hydroxyapatite microparticles, Polym. Degrad. Stab. 167 (2019) 21–32, https://doi.org/10.1016/j.polymdegradstab.2019.06.017.

[116] P. Tyagi, S.A. Catledge, A. Stanishevsky, V. Thomas, Y.K. Vohra, Nanomechanical properties of electrospun composite scaffolds based on polycaprolactone and hydroxyapatite, J. Nanosci. Nanotechnol. 9 (2009) 4839–4845, https://doi.org/10.1166/jnn.2009.1588.

[117] K. Saeed, S.-Y. Park, H.-W. Lee, J.-B. Baek, W.-S. Huh, Preparation of electrospun nanofibers of carbon nanotube/polycaprolactone nanocomposite, Polymer 47 (2006) 8019–8025, https://doi.org/10.1016/j.polymer.2006.09.012.

[118] G. Narayanan, B.S. Gupta, A.E. Tonelli, Enhanced mechanical properties of poly (ε-caprolactone) nanofibers produced by the addition of non-stoichiometric inclusion complexes of poly (ε-caprolactone) and α-cyclodextrin, Polymer 76 (2015) 321–330, https://doi.org/10.1016/j.polymer.2015.08.045.

[119] R. Zhang, P.X. Ma, Porous poly(L-lactic acid)/apatite composites created by the biomimetic process, J. Biomed. Mater. Res. 45 (4) (1999) 285–293, https://doi.org/10.1002/(SICI)1097-4636(19990615)45:4<285::AID-JBM2>3.0.CO;2-2.

[120] C. Wu, Y. Ramaswamy, Y. Zhu, R. Zheng, R. Appleyard, A. Howard, H. Zreiqat, The effect of mesoporous bioactive glass on the physiochemical, biological and drug-release properties of poly(dl-lactide-co-glycolide) films, Biomaterials 30 (12) (2009) 2199–2208, https://doi.org/10.1016/j.biomaterials.2009.01.029.

[121] S.N. Gorodzha, A.R. Muslimov, D.S. Syromotina, A.S. Timin, N.Y. Tcvetkov, K.V. Lepik, A.V. Petrova, M.A. Surmeneva, D.A. Gorin, G.B. Sukhorukov, R.A. Surmeneva, A comparison study between electrospun polycaprolactone andpiezoelectric poly(3-hydroxybutyrate-co-3-hydroxyvalerate)scaffolds for bone

[122] W. TheinHan, M.D. Weir, C.G. Simon, H.H. Xu, Non-rigid calcium phosphate cement containing hydrogel microbeads and absorbable fibres seeded with umbilical cord stem cells for bone engineering, J. Tissue Eng. Regenerat. Med. 7 (10) (2012) 777–787, https://doi.org/10.1002/term.1466.

[123] M. Soltani, M. Yousefpour, Z. Taherian, Porous fluorhydroxyapatite-magnesium-gelatin novel composite scaffold based on the freeze-drying mechanism for bone tissue engineering application, Mater. Lett. 244 (2019) 195–198, https://doi.org/10.1016/j.matlet.2019.02.088.

[124] S.W. Crowder, D. Prasai, R. Rath, D.A. Balikov, H. Bae, K.I. Bolotin, H.J. Sung, Three-dimensional graphene foams promote osteogenic differentiation of human mesenchymal stem cells, Nanoscale 5 (2013) 4171–4176, https://doi.org/10.1039/c3nr00803g.

[125] S. Kang, J.B. Park, T.J. Lee, S. Ryud, S.H. Bhange, W.G. Laf, M.K. Noh, B.H. Hong, B.S. Kim, Covalent conjugation of mechanically stiff graphene oxide flakes to three-dimensional collagen scaffolds for osteogenic differentiation of human mesenchymal stem cells, Carbon 83 (2015) 162–172, https://doi.org/10.1016/j.carbon.2014.11.029.

[126] C. Wu, Y. Zhang, Y. Zhu, T. Friis, Y. Xiao, Structure-property relationships of silk-modified mesoporous bioglass scaffolds, Biomaterials 31 (13) (2010) 3429–3438, https://doi.org/10.1016/j.biomaterials.2010.01.061.

[127] J. Chen, H. Chen, P. Li, H. Diao, S. Zhu, L. Dong, R. Wang, T. Guo, J. Zhao, J. Zhang, Simultaneous regeneration of articular cartilage and subchondral bone in vivo using MSCs induced by a spatially controlled gene delivery system in bilayered integrated scaffolds, Biomaterials 32 (21) (2011) 4793–4805, https://doi.org/10.1016/j.biomaterials.2011.03.041.

[128] A.L. Torres, V.M. Gaspar, I.R. Serra, G.S. Diogo, R. Fradique, A.P. Silva, I.J. Correia, Bioactive polymeric–ceramic hybrid 3D scaffold for application in bone tissue regeneration, Mater. Sci. Eng. C 33 (7) (2013) 4460–4469, https://doi.org/10.1016/j.msec.2013.07.003.

[129] X. Liu, C. Ding, P.K. Chu, Mechanism of apatite formation on wollastonite coatings in simulated body fluids, Biomaterials 25 (10) (2004) 1755–1761, https://doi.org/10.1016/j.biomaterials.2003.08.024.

[130] A. Tache, L. Gan, D. Deporter, R.M. Pilliar, Effect of surface chemistry on the rate of osseointegration of sintered porous-surfaced Ti-6Al-4V implants, Int. J. Oral Maxillofac. Implant. 19 (1) (2004) 19–29.

[131] P. Li, Biomimetic nano-apatite coating capable of promoting bone ingrowth, J. Biomed. Mater. Res. A 66 (1) (2003) 79–85, https://doi.org/10.1002/jbm.a.10519.

[132] A. Rifai, N. Tran, D.W. Lau, A. Elbourne, H. Zhan, A.D. Stacey, E.L.H. Mayes, A. Sarker, E.P. Ivanova, R.J. Crawford, P.A. Tran, B.C. Gibson, A.D. Greentree, E. Pirogova, K. Fox, Polycrystalline diamond coating of additively manufactured titanium for biomedical applications, ACS Appl. Mater. Interfaces 10 (10) (2018) 8474–8484, https://doi.org/10.1021/acsami.7b18596.

[133] M. Surmeneva, A. Lapanje, E. Chudinova, A. Ivanova, A. Koptyug, K. Loza, O. Prymak, M. Epple, F. Ennen-Roth, M. Ulbricht, T. Rijavec, R. Surmenev, Decreased bacterial colonization of additively manufactured Ti6Al4V metallic scaffolds with immobilized silver and calcium phosphate nanoparticles, Appl. Surf. Sci. 480 (2019) 822–829, https://doi.org/10.1016/j.apsusc.2019.03.003.

[134] S. Wust, M.E. Godla, R. Muller, S. Hofmann, Tunable hydrogel composite with two-step processing in combination with innovative hardware upgrade for cell-based three-dimensional bioprinting, Acta Biomater. 10 (2) (2014) 630–640, https://doi.org/10.1016/j.actbio.2013.10.016.

[135] C. Chang, N. Peng, M. He, Y. Teramoto, Y. Nishio, L. Zhang, Fabrication and properties of chitin/hydroxyapatite hybrid hydrogels as scaffold nano-materials, Carbohydr. Polym. 1 (1) (2013) 7–13, https://doi.org/10.1016/j.carbpol.2012.07.070.

[136] S. Maji, T. Agarwal, J.D. Tapas, K. Maiti, Development of gelatin/carboxymethyl chitosan/nano-hydroxyapatite composite 3D macroporous scaffold for bone tissue engineering applications, Carbohydr, Polymers 189 (2018) 115–125, https://doi.org/10.1016/j.carbpol.2018.01.104.

[137] Y. Huang, X. Zhang, A. Wua, H. Xu, An injectable nano-hydroxyapatite (n-HA)/glycol chitosan (G-CS)/hyaluronic acid (HyA) composite hydrogel for bone tissue engineering, RSC Adv. 6 (2016) 33529–33536, https://doi.org/10.1039/C5RA26160K.

[138] S. Saravanan, Anjali Chawla, M. Vairamani, T.P. Sastry, K.S. Subramanian, N. Selvamurugan, Scaffolds containing chitosan, gelatin and graphene oxide for bone tissue regeneration in vitro and in vivo, Int. J. Biol. Macromol. 104 (2017) 1975–1985, https://doi.org/10.1016/j.ijbiomac.2017.01.034.

[139] A. Tripathi, S. Saravanan, S. Pattnaik, A. Moorthi, N.C. Partridge, N. Selvamurugan, Bio-composite scaffolds containing chitosan/nano-hydroxyapatite/nano-copper-zinc for bone tissue engineering, Int. J. Biol. Macromol. 50 (2012) 294–299, https://doi.org/10.1016/j.ijbiomac.2011.11.013.

[140] Y. Gao, W. Shao, W. Qian, J. He, Y. Zhou, K. Qi, L. Wang, S. Cui, R. Wang, Biomineralized poly (l-lactic-co-glycolic acid)-tussah silk fibroin nanofiber fabric with hierarchical architecture as a scaffold for bone tissue engineering, Mater. Sci. Eng. C 84 (1) (2018) 195–207, https://doi.org/10.1016/j.msec.2017.11.047.

[141] S. Kwak, A. Haider, K.C. Gupta, S. Kim, I.-K. Kang, Micro/nano multilayered scaffolds of PLGA and collagen by alternately electrospinning for bone tissue engineering, Nanoscale Res. Lett. 11 (2016) 323, https://doi.org/10.1186/s11671-016-1532-4.

[142] S.T. Bendtsen, S.P. Quinnell, M. Wei, Development of a novel alginate-polyvinyl alcohol-hydroxyapatite hydrogel for 3D bioprinting bone tissue-engineered scaffolds, J. Biomed. Mater. Res. A 105 (5) (2017) 1457–1468, https://doi.org/10.1002/jbm.a.36036.

[143] A.I. Rezk, A.R. Unnithan, C.H. Park, C.S. Kim, Rational design of bone extra-cellular matrix mimicking tri-layered composite nanofibers for bone tissue regeneration, Chem. Eng. J. 350 (2018) 812–823, https://doi.org/10.1016/j.cej.2018.05.185.

[144] Z. Chen, Y. Song, J. Zhang, W. Liu, J. Cui, H. Li, F. Chen, Laminated electrospun nHA/PHB-composite scaffolds mimicking bone extracellular matrix for bone tissue engineering, Mater. Sci. Eng. C 72 (2017) 341–351, https://doi.org/10.1016/j.msec.2016.11.070.

[145] K. Kaur, K.J. Singh, V. Anand, G. Bhatia, R. Kaur, M. Kaur, L. Nim, D.S. Arora, Scaffolds of hydroxyl apatite nanoparticles disseminated in 1,6-diisocyanato-hexane-extended poly(1,4-butylene succinate)/poly(methyl methacrylate) for bone tissue engineering, Mater. Sci. Eng. C 71 (2017) 780–790, https://doi.org/10.1016/j.msec.2016.10.055.

[146] H. Eslami, H. Azimi Lisar, T.S. Jafarzadeh Kashi, M. Tahriri, M. Ansari, T. Rafiei, F. Bastami, A. Shahin-Shamsabadi, F. Mashhadi Abbas, L. Tayebi, Poly(lactic-co-glycolic acid)(PLGA)/TiO2 nanotube bioactive composite as a novel scaffold for bone tissue engineering: in vitro and in vivo studies, Biologicals 53 (2018) 51–62, https://doi.org/10.1016/j.biologicals.2018.02.004.

[147] B.K. Shrestha, S. Shrestha, A.P. Tiwari, J.-I. Kim, S.W. Ko, H.-J. Kim, C.H. Park, C.S. Kim, Bio-inspired hybrid scaffold of zinc oxide-functionalized multi-wall carbon nanotubes reinforced polyurethane nanofibers for bone tissue engineering, Mater. Des. 133 (2017) 69–81, https://doi.org/10.1016/j.matdes.2017.07.049.

[148] A.I. Rezk, H.M. Mousa, J. Lee, C.H. Park, C.S. Kim, Composite PCL/HA/simvastatin electrospun nanofiber coating on biodegradable Mg alloy for orthopaedic implant application, J. Coat. Technol. Res. 16 (2) (2019) 477–489, https://doi.org/10.1007/s11998-018-0126-8.

[149] W. Nie, C. Peng, X. Zhou, L. Chen, W. Wang, Y. Zhang, P.X. Ma, C. He, Three-dimensional porous scaffold by self-assembly of reduced graphene oxide and nano-hydroxyapatite composites for bone tissue engineering, Carbon 116 (2017) 325–337, https://doi.org/10.1016/j.carbon.2017.02.013.

[150] Y. Fu, L. Liu, R. Cheng, W. Cui, ECM decorated electrospun nanofiber for improving bone tissue regeneration, Polymers 10 (3) (2018) 272, https://doi.org/10.3390/polym10030272.

[151] P. Lee, K. Tran, W. Chang, Y.-L. Fang, G. Zhou, R. Junka, N.B. Shelke, X. Yu, S.G. Kumbar, Bioactive polymeric scaffolds for osteochondral tissue engineering: in vitro evaluation of the effect of culture media on bone marrow stromal cells, Polym. Adv. Technol. 26 (2015) 1476–1485, https://doi.org/10.1002/pat.3680.

[152] P. Lee, K. Tran, G. Zhou, A. Bedi, N.B. Shelke, X. Yu, S.G. Kumbar, Guided differentiation of bone marrow stromal cells on co-cultured cartilage and bone scaffolds, Soft Matter 11 (2015) 7648–7655, https://doi.org/10.1039/C5SM01909E.

[153] J.E. Mayer, T. Shinoka, D. Shum-Tim, Tissue engineering of cardiovascular structures, Curr. Opin. Cardiol. 12 (6) (1997) 528–532, https://doi.org/10.1097/00001573-199711000-00005.

[154] F. Oberpenning, J. Meng, J.J. Yoo, A. Atala, De novo reconstitution of a functional mammalian urinary bladder by tissue engineering, Nat. Biotechnol. 17 (2) (1999) 149–155, https://doi.org/10.1038/6146.

[155] E. Tziampazis, A. Sambanis, Tissue engineering of a bioartificial pancreas: modelling the cell environment and device function, Biotechnol. Prog. 11 (2) (1995) 115–126, https://doi.org/10.1021/bp00032a001.

[156] K.T. Santhosh, A. Alizadeh, S. Karimi-Abdolrezaee, Design and optimization of PLGA microparticles for controlled and local delivery of neuregulin-1 in traumatic spinal cord injury, J. Control. Release 261 (2017) 147–162, https://doi.org/10.1016/j.jconrel.2017.06.030.

[157] S. Pieretti, A.P. Ranjan, A. Di Giannuario, A. Mukerjee, F. Marzoli, R. Di Giovannandrea, J.K. Vishwanatha, Curcumin-loaded poly(D, L-lactide-co-glycolide) nanovesicles induce antinociceptive effects and reduce pronociceptive cytokine and BDNF release in the spinal cord after acute administration in mice, Colloids Surf., B 158 (2017) 379–386, https://doi.org/10.1016/j.colsurfb.2017.07.027.

[158] Y.J. Che, L. Chen, G.H. Lv, X.B. Wang, In situ gel delivery system of methylprednisolone for post-traumatic spinal injuries, J. Biomater. Tissue Eng. 5 (7) (2015) 552–556, https://doi.org/10.1166/jbt.2015.1347.

[159] B.L. Du, C.G. Zeng, W. Zhang, D.P. Quan, E.A. Ling, Y.S. Zeng, A comparative study of gelatin sponge scaffolds and PLGA scaffolds transplanted to the completely transected spinal cord of rat, J. Biomed. Mater. Res. A 102 (6) (2014) 1715–1725, https://doi.org/10.1002/jbm.a.34835.

[160] A. Murua, E. Herran, G. Orive, M. Igartua, F.J. Blanco, J.L. Pedraz, R. M Hernández, Design of a composite drug delivery system to prolong the functionality of cell-based scaffolds, Int. J. Pharmaceutics 407 (1–2) (2011) 142–150, https://doi.org/10.1016/j.ijpharm.2010.11.022.

[161] O. Janoušková, Synthetic polymer scaffolds for soft tissue engineering, Physiol. Res. 67 (2) (2018) S335–S348, https://doi.org/10.33549/physiolres.933983.

[162] K.J. Aviss, J.E. Gough, S. Downes, Aligned electrospun polymer fibres for skeletal muscle regeneration, Eur. Cells Mater. 19 (2010) 193–204, https://doi.org/10.22203/eCM.v019a19.

[163] M.C. Chen, Y.C. Sun, Y.H. Chen, Electrically conductive nanofibers with highly oriented structures and their potential application in skeletal muscle tissue engineering, Acta Biomater. 9 (2013) 5562–5572, https://doi.org/10.1016/j.actbio.2012.10.024.

[164] T. Li, L. Tian, S. Liao, X. Ding, S.A. Irvine, S. Ramakrishna, Fabrication, mechanical property and in vitro evaluation of poly (L-lactic acid-co-ε-caprolactone) core-shell nanofiber scaffold for tissue engineering, J. Mech. Behav. Biomed. Mater. 98 (2019) 48–57, https://doi.org/10.1016/j.jmbbm.2019.06.003.

[165] M.S. Islam, B.C. Ang, A. Andriyana, A.M. Afifi, A review on fabrication of nanofibers via electrospinning and their applications, SN Appl. Sci. 1 (2019) 1248, https://doi.org/10.1007/s42452-019-1288-4.

[166] X. Li, C. Yang, L. Li, J. Xiong, L. Xie, B. Yang, M. Yu, L. Feng, Z. Jiang, W. Guo, W. Tian, A therapeutic strategy for spinal cord defect: human dental follicle cells combined with aligned PCL/PLGA electrospun material, BioMed Res. Int. 2015 (2015) 197183, https://doi.org/10.1155/2015/197183.

[167] C.Y. Wang, J.J. Liu, C.Y. Fan, X.M. Mo, H.J. Ruan, F.F. Li, The effect of aligned core-shell nanofibres delivering NGF on the promotion of sciatic nerve regeneration, J. Biomater. Sci. Polym. Ed. 23 (1–4) (2012) 167–184, https://doi.org/10.1163/092050610X545805.

[168] E.J. Laurilliard, K.L. Lee, J.A. Cooper, Characterization and Evaluation of Fabricated poly(L-Lactic) Acid Core Fibres for Ligament Fascicle Development, 41st Annual Northeast Biomedical Engineering Conference (NEBEC), (2015), pp. 1–2, https://doi.org/10.1109/NEBEC.2015.7117108.

[169] D.A. Sánchez-Téllez, L. Téllez-Jurado, L.M. Rodríguez-Lorenzo, Hydrogels for cartilage regeneration, from polysaccharides to hybrids, Polymers 9 (2017) 671, https://doi.org/10.3390/polym9120671.

[170] H.D. Kim, Y. Lee, Y. Kim, Y. Hwang, N.S. Hwang, Biomimetically reinforced polyvinyl alcohol-based hybrid scaffolds for cartilage tissue engineering, Polymers 9 (12) (2017) 655, https://doi.org/10.3390/polym9120655.

[171] B.V. Sridhar, N.R. Doyle, M.A. Randolph, K.S. Anseth, Covalently tethered TGF-β1 with encapsulated chondrocytes in a PEG hydrogel system enhances extracellular matrix production, J. Biomed. Mater. Res. A 102 (12) (2014) 4464–4472, https://doi.org/10.1002/jbm.a.35115.

[172] T. Guo, C.G. Lim, M. Noshin, J.P. Ringel, J.P. Fisher, 3D printing bioactive PLGA scaffolds using DMSO as a removable solvent, Bioprinting 10 (2018) e00038, , https://doi.org/10.1016/j.bprint.2018.e00038.

[173] X. Jing, H.-Y. Mi, H.-X. Huang, L.-S. Turning, Shape memory thermoplastic polyurethane (TPU)/poly(ε-caprolactone) (PCL) blends as self-knotting sutures, J. Mech. Behav. Biomed. Mater. 64 (2016) 94–103, https://doi.org/10.1016/j.jmbbm.2016.07.023.

[174] J.W. Lee, J.Y. Kim, D.-W. Cho, Solid free-form fabrication technology and its application to bone tissue engineering, Int. J. Stem Cells 3 (2) (2010) 85–95 https://www.ncbi.nlm.nih.gov/pmc/articles/PMC4021802/.

[175] D. Putnam, The heart of the matter, Nat. Mater. 7 (2008) 836–837, https://doi.org/10.1038/nmat2309.

[176] A.J. Rufaihah, C. Yasa, Vaibavi, S. Ramanujam, S.C. Arularasu, T. Kofidis, M.O. Guler, A.B. Tekinay, Angiogenic peptide nanofibers repair cardiac tissue defect after myocardial infarction, Acta Biomater. 58 (2017) 102–112, https://doi.org/10.1016/j.actbio.2017.06.009.

[177] G. Uzunalli, Y. Tomas, T. Delibasi, O. Yasa, S. Mercan, M.O. Guler, A.B. Tekinay, Improving pancreatic islet in vitro functionality and transplantation efficiency by using heparin mimetic peptide nanofiber gels, Acta Biomater. 22 (2015) 8–18, https://doi.org/10.1016/j.actbio.2015.04.032.

[178] T. Fernández-Muiños, L. Recha-Sancho, P. López-Chicón, C. Castells-Sala, A. Mata, C.E. Semino, Bimolecular based heparin and self-assembling hydrogel for tissue engineering applications, Acta Biomater. 16 (1) (2015) 35–48, https://doi.org/10.1016/j.actbio.2015.01.008.

[179] Y. Li, F. Wang, H. Cui, Peptide-based supramolecular hydrogels for delivery of biologics, Bioeng. Transl. Med. 1 (3) (2016) 306–322, https://doi.org/10.1002/btm2.10041.

[180] S.M. Vickers, L.S. Squitieri, M. Spector, Effects of cross-linking type II collagen-GAG scaffolds on chondrogenesis in vitro: dynamic pore reduction promotes cartilage formation, Tissue Eng. 12 (2006) 1345–1355, https://doi.org/10.1089/ten.2006.12.1345.

[181] Y. Pang, H.P. Greisler, Using a type I collagen-based system to understand cell-scaffold interactions and to deliver chimeric collagen-binding growth factors for vascular tissue engineering, J. Investig. Med. Off. Publ. Am. Fed. Clin. Res. 58 (2010) 845–848 10.231/JIM.0b013e3181ee81f7.

[182] S. Han, B. Wang, W. Jin, Z. Xiao, X. Li, W. Ding, M. Kapur, B. Chen, B. Yuan, T. Zhu, H. Wang, J. Wang, Q. Dong, W. Liang, J. Dai, The linear-ordered collagen scaffold-BDNF complex significantly promotes functional recovery after completely transected spinal cord injury in canine, Biomaterials 41 (2015) 89–96, https://doi.org/10.1016/j.biomaterials.2014.11.031.

[183] X. Chen, Y. Fan, Z. Xiao, X. Li, B. Yang, Y. Zhao, X. Hou, S. Han, J. Dai, Promotion of transplanted collagen scaffolds combined with brain-derived neurotrophic factor for axonal regeneration and motor function recovery in rats after transected spinal cord injury, Chin. J. Reparative Reconstr. Surg. 32 (6) (2018) 650–659, https://doi.org/10.7507/1002-1892.201803094.

[184] E. Serena, M. Flaibani, S. Carnio, L. Boldrin, L. Vitiello, P. De Coppi, N. Elvassore, Electrophysiologic stimulation improves myogenic potential of muscle precursor cells grown in a 3D collagen scaffold, Neurol. Res. 30 (2008) 207–214, https://doi.org/10.1179/174313208X281109.

[185] D.P. Bhattarai, L.E. Aguilar, C.H. Park, C.S. Kim, A review on properties of natural and synthetic based electrospun fibrous materials for bone tissue engineering, Membranes 8 (2018) 62, https://doi.org/10.3390/membranes8030062.

[186] M. Onuma-Ukegawa, K. Bhatt, T. Hirai, H. Kaburagi, S. Saotome, Y. Wakabayashi, S. Ichinose, K. Shinomiya, A. Okawa, M. Enomoto, Bone marrow stromal cells combined with a honeycomb collagen sponge facilitate neurite elongation in bitro and neural restoration in the hemisected rat spinal cord, Cell Transplant. 24 (7) (2015) 1283–1297, https://doi.org/10.3727/096368914X682134.

[187] T.C. Tseng, L. Tao, F.Y. Hsieh, Y. Wei, I.M. Chiu, S.H. Hsu, An injectable, self-healing hydrogel to repair the central nervous system, Adv. Mater. 27 (2015) 3518–3524, https://doi.org/10.1002/adma.201500762.

[188] H. Mackova, Z. Plichta, V. Proks, I. Kotelnikov, J. Kucka, H. Hlidkova, D. Horak, S. Kubinova, J. Jirakova, RGDS- and SIKVAVS-modifiedsuperporous poly(2-hydroxyethyl methacrylate) scaffolds for tis-sue engineering applications, Macromol.

Biosci. 16 (2016) 1621–1631, https://doi.org/10.1002/mabi.201600159.

[189] K. Zaviskova, D. Tukmachev, J. Dubisova, I. Vackova, A. Hejcl, J. Bystronova, M. Pravda, I. Scigalkova, R. Sulakova, V. Velebny, L. Wolfova, S. Kubinova, Injectable hydroxyphenyl derivative of hyaluronic acid hydrogel modifiedwith RGD as scaffold for spinal cord injury repair, J. Biomed. Mater. Res. A 106 (4) (2017) 1129–1140, https://doi.org/10.1002/jbm.a.36311.

[190] R. Almeida, D.P. Vasconcelos, R.M. Goncalves, M.A. Barbosa, Enhanced mesenchymal stromal cell recruitment via natural killer cells by incorporation of inflammatory signals in biomaterials, J. R. Soc. Interface 9 (2012) 261–271, https://doi.org/10.1098/rsif.2011.0357.

[191] M. Mata, L. Milian, M. Oliver, J. Zurriaga, M. Sancho-Tello, J.J.M. de Llano, C. Carda, In vivo articular cartilage regeneration using human dental pulp stem cells cultured in an alginate scaffold: a preliminary study, Stem Cell. Int. (2017) e8309256, , https://doi.org/10.1155/2017/8309256 2017.

[192] Y. Wang, D.J. Blasioli, H.-J. Kim, H.S. Kim, D.L. Kaplan, Cartilage tissue engineering with silk scaffolds and human articular chondrocytes, Biomaterials 27 (2006) 4434–4442, https://doi.org/10.1016/j.biomaterials.2006.03.050.

[193] T. Kardestuncer, M. McCarthy, V. Karageorgiou, D. Kaplan, G. Gronowicz, RGD-tethered silk substrate stimulates the differentiation of human tendon cells, Clin. Orthop. Relat. Res. 448 (2006) 234–239, https://doi.org/10.1097/01.blo.0000205879.50834.fe.

[194] Z.-X. Cai, X.-M. Mo, K.-H. Zhang, L.-P. Fan, A.-l. Yin, C.-l. He, Fabrication of chitosan/silk fibroin composite nanofibers for wound dressing applications, Int. J. Mol. Sci. 11 (2010) 3529–3539, https://doi.org/10.3390/ijms11093529.

[195] Z. Zhu, Y.-M. Wang, J. Yang, X.-S. Luo, Hyaluronic acid: a versatile biomaterial in tissue engineering, Plast. Aesthet. Res. 4 (2017) 219–227, https://doi.org/10.20517/2347-9264.2017.71.

[196] I.P. Monteiro, A. Shukla, A.P. Marques, R.L. Reis, P.T. Hammond, Spray-assisted layer-by-layer assembly on hyaluronic acid scaffolds for skin tissue engineering, J. Biomed. Mater. Res. A. 103 (2015) 330–340, https://doi.org/10.1002/jbm.a.35178.

[197] C.-W. Lin, Y.-K. Chen, K.-C. Tang, K.-C. Yang, N.-C. Cheng, J. Yu, Keratin scaffolds with human adipose stem cells: physical and biological effects toward wound healing, J. Tissue Eng. Regenerat. Med. 13 (6) (2019) 1044–1058, https://doi.org/10.1002/term.2855.

[198] Y.Z. Zhang, J. Venugopal, Z.M. Huang, C.T. Lim, S. Ramakrishna, Crosslinking of the electrospun gelatin nanofibers, Polymer 47 (2006) 2911–2917, https://doi.org/10.1016/j.polymer.2006.02.046.

[199] Y. Elsayed, C. Lekakou, F. Labelled, P. Tomlins, Smooth muscle tissue engineering in crosslinked electrospun gelatin scaffolds, J. Biomed. Mater. Res. A (2015) 313–321, https://doi.org/10.1002/jbm.a.35565.

[200] F.Y. Hsu, Y.S. Hung, H.M. Liou, C.H. Shen, Electrospun hyaluronate-collagen nanofibrous matrix and the effects of varying the concentration of hyaluronate on the characteristics of foreskin fibroblast cells, Acta Biomater. 6 (6) (2010) 2140–2147, https://doi.org/10.1016/j.actbio.2009.12.023.

[201] Q. Zhang, B. Shi, J. Ding, L. Yan, J.P. Thawani, C. Fu, X. Chen, Polymer scaffolds facilitate spinal cord injury repair, Acta Biomater. 88 (2019) 57–77, https://doi.org/10.1016/j.actbio.2019.01.056.

[202] S. Stratton, N.B. Shelke, K. Hoshino, S. Rudraiah, S.G. Kumbar, Bioactive polymeric scaffolds for tissue engineering, Bioact. Mater. 1 (2) (2016) 93–108, https://doi.org/10.1016/j.bioactmat.2016.11.001.

[203] J.-H. Shim, J.-S. Lee, J.Y. Kim, D.-W. Cho, Bioprinting of a mechanically enhanced three-dimensional dual cell-laden construct for osteochondral tissue engineering using a multi-head tissue/organ building system, J. Micromech. Microeng. 22 (2012) 085014, , https://doi.org/10.1088/0960-1317/22/8/085014.

[204] S.C. Neves, L.S.M. Teixeira, L. Moroni, R.L. Reis, C.A. Van Blitterswijk, N.M. Alves, M. Karperien, J.F. Mano, Chitosan/Poly (ε-caprolactone) blend scaffolds for cartilage repair, Biomaterials 32 (2011) 1068–1079, https://doi.org/10.1016/j.biomaterials.2010.09.073.

[205] H. Kenar, C.Y. Ozdogan, C. Dumlu, E. Doger, G.T. Kose, V. Hasirci, Microfibrous scaffolds from poly(l-lactide-co-ε-caprolactone) blended with xeno-free collagen/hyaluronic acid for improvement of vascularization in tissue engineering applications, Mater. Sci. Eng. C 97 (2019) 31–44, https://doi.org/10.1016/j.msec.2018.12.011.

[206] C.-H. Yao, C.-Y. Lee, C.-H. Huang, Y.-S. Chen, K.-Y. Chen, Novel bilayer wound dressing based on electrospun gelatin/keratin nanofibrous mats for skin wound repair, Mater. Sci. Eng. C Mater. Biol. Appl. 79 (2017) 533–540, https://doi.org/10.1016/j.msec.2017.05.076.

[207] Y.J. Wen, S.K. Yu, Y.H. Wu, R.K. Ju, H. Wang, Y.J. Liu, Y. Wang, Q.Y. Xu, Spinal cord injury repair by implantation of the structured hyaluronic acid scaffold with PLGA microspheres in the rat, Cell Tissue Res. 364 (1) (2016) 17–28, https://doi.org/10.1007/s00441-015-2298-1.

[208] T. Xu, K.W. Binder, M.Z. Albanna, D. Dice, W. Zhao, J.J. Yoo, A. Atala, Hybrid printing of mechanically and biologically improved constructs for cartilage tissue engineering applications, Biofabrication 5 (1) (2013) 015001, , https://doi.org/10.1088/1758-5082/5/1/015001.

[209] D.B. Kolesky, K.A. Homan, M.A. Skylar-Scott, J.A. Lewis, Three-dimensional bioprinting of thick vascularized tissues, Proc. Natl. Acad. Sci. U.S.A. 113 (12) (2016) 3179–3184, https://doi.org/10.1073/pnas.1521342113.

[210] C. Colosi, S.R. Shin, V. Manoharan, S. Massa, M. Costantini, A. Barbetta, M.R. Dokmeci, M. Dentini, A. Khademhosseini, Microfluidic bioprinting of heterogeneous 3D tissue constructs using low-viscosity bioink, Adv. Mater. 28 (4) (2016) 677–684, https://doi.org/10.1002/adma.201503310.

[211] B. Duan, E. Kapetanovic, L.A. Hockaday, J.T. Butcher, Three-dimensional printed trileaflet valve conduits using biological hydrogels and human valve interstitial cells, Acta Biomater. 10 (5) (2014) 1836–1846, https://doi.org/10.1016/j.actbio.2013.12.005.

[212] A. Skardal, M. Devarasetty, H.W. Kang, I. Mead, C. Bishop, T. Shupe, S.J. Lee, J. Jackson, J. Yoo, S. Soker, A. Atala, A hydrogel bioink toolkit for mimicking native tissue biochemical and mechanical properties in bioprinted tissue constructs, Acta Biomater. 25 (2015) 24–34, https://doi.org/10.1016/j.actbio.2015.07.030.

[213] S. Huang, B. Yao, J. Xie, X. Fu, 3D bioprinted extracellular matrix mimics facilitate directed differentiation of epithelial progenitors for sweat gland regeneration, Acta Biomater. 32 (2016) 170–177, https://doi.org/10.1016/j.actbio.2015.12.039.

[214] M. Kesti, C. Eberhardt, G. Pagliccia, D. Kenkel, D. Grande, A. Boss, M. Zenobi-Wong, Bioprinting complex cartilaginous structures with clinically compliant biomaterials, Adv. Funct. Mater. 25 (48) (2015) 7406–7417, https://doi.org/10.1002/adfm.201503423.

[215] M. Yeo, J.S. Lee, W. Chun, G.H. Kim, An innovative collagen-based cell-printing method for obtaining human adipose stem cell-laden structures consisting of core-sheath structures for tissue engineering, Biomacromolecules 17 (4) (2016) 1365–1375, https://doi.org/10.1021/acs.biomac.5b01764.

[216] M. Severa, M. Turkyilmaz, C. Sevinc, A. Cakir, B. Ocalan, M. Cansev, M.O. Guler, A.B. Tekinay, Regenerative effects of peptide nanofibers in an experimental model of Parkinson's disease, Acta Biomater. 46 (2016) 79–90, https://doi.org/10.1016/j.actbio.2016.09.011.

[217] J.D. Patient, H. Hajiali, K. Harris, B. Abrahamsson, C. Tannergren, L.J. White, A.M. Ghaemmaghami, P.M. Williams, C.J. Roberts, F.R.A.J. Rose, Nanofibrous scaffolds support a 3D in vitro permeability model of the human intestinal epithelium, Front. Pharmacol. 10 (2019) 456, https://doi.org/10.3389/fphar.2019.00456.

[218] A.P. Tiwari, T.I. Hwang, J.M. Oh, B. Maharjan, S. Chun, B.S. Kim, M.K. Joshi, C.H. Park, C.S. Kim, pH/nir-responsive polypyrrole-functionalized fibrous localized drug-delivery platform for synergistic cancer therapy, ACS Appl. Mater. Interfaces 10 (24) (2018) 20256–20270, https://doi.org/10.1021/acsami.7b17664.

[219] J.I. Kim, J.Y. Kim, C.H. Park, Fabrication of transparent hemispherical 3D nanofibrous scaffolds with radially aligned patterns via a novel electrospinning method, Sci. Rep. 8 (2018) 3424, https://doi.org/10.1038/s41598-018-21618-0.

[220] K. Byoung Soo, L. Jung-Seob, G. Ge, C. Dong-Woo, Direct 3D cell-printing of human skin with functional transwell system, Biofabrication 9 (2) (2017) 025034, , https://doi.org/10.1088/1758-5090/aa71c8.

[221] V. Albright, M. Xu, A. Palanisamy, J. Cheng, M. Stack, B. Zhang, A. Jayaraman, S.A. Sukhishvili, H. Wang, Micelle-coated, hierarchically structured nanofibers with dual-release capability for accelerated wound healing and infection control, Adv. Healthc. Mater. 7 (11) (2018) e1800132, , https://doi.org/10.1002/adhm.201800132.

[222] N.W. Garrigues, D. Little, J. Sanchez-Adams, D.S. Ruch, F. Guilak, Electrospun cartilage-derived matrix scaffolds for cartilage tissue engineering, J. Biomed. Mater. Res. A 102 (11) (2014) 3998–4008, https://doi.org/10.1002/jbm.a.35068.

[223] S. Hackelberg, S.J. Tuck, L. He, A. Rastogi, C. White, L. Liu, D.M. Prieskorn, R.J. Miller, C. Chan, B.R. Loomis, J.M. Corey, J.M. Miller, R.K. Duncan, Nanofibrous scaffolds for the guidance of stem cell-derived neurons for auditory nerve regeneration, PLoS One 12 (7) (2017) e0180427, , https://doi.org/10.1371/journal.pone.0180427.

[224] Y.H. Gong, L.J. He, J. Li, Q.L. Zhou, Z.W. Ma, C.Y. Gao, J.C. Shen, Hydrogel-filled polylactide porous scaffolds for cartilage tissue engineering, J. Biomed. Mater. Res. B. 82 (2007) 192–204, https://doi.org/10.1002/jbm.b.30721.

[225] A. Sciancalepore, M. Moffa, S. Carluccio, L. Romano, G.S. Netti, C. Prattichizzo, D. Pisignano, Bioactive nanofiber matrices functionalized with fibronectin-mimetic peptides driving the alignment and tubular commitment of adult renal stem cells, Macromol. Chem. Phys. 217 (2) (2016) 199–212, https://doi.org/10.1002/macp.201500370.

[226] B. Pei, W. Wang, Y. Fan, X. Wang, F. Watari, X. Li, Fiber-reinforced scaffolds in soft tissue engineering, Regen. Biomater. 4 (4) (2017) 257–268, https://doi.org/10.1093/rb/rbx021.

[227] J. Zhou, C. Xu, G. Wu, X. Cao, L. Zhang, Z. Zhai, Z. Zheng, X. Chen, Y. Wang, In vitro generation of osteochondral differentiation of human marrow mesenchymal stem cells in novel collagen-hydroxyapatite layered scaffolds, Acta Biomater. 7 (11) (2011) 3999–4006, https://doi.org/10.1016/j.actbio.2011.06.040.

[228] D. Xue, Q. Zheng, C. Zong, Q. Li, H. Li, S. Qian, B. Zhang, L. Yu, Z. Pan, Osteochondral repair using porous poly(lactide-co-glycolide)/nano-hydroxyapatite hybrid scaffolds with undifferentiated mesenchymal stem cells in a rat model, J. Biomed. Mater. Res. 94A (1) (2010) 259–270, https://doi.org/10.1002/jbm.a.32691.

[229] X. Zhou, M. Nowicki, H. Cui, W. Zhu, X. Fang, S. Miao, S.-J. Lee, M. Keidar, L.G. Zhang, 3D bioprinted graphene oxide-incorporated matrix for promoting chondrogenic differentiation of human bone marrow mesenchymal stem cells, Carbon 116 (2017) 615–624, https://doi.org/10.1016/j.carbon.2017.02.049.

[230] S.M. Hong, J.W. Kim, J.C. Knowles, M.S. Gong, Facile preparation of antibacterial, highly elastic silvered polyurethane nanofiber fabrics using silver carbamate and their dermal wound healing properties, J. Biomater. Appl. 31 (7) (2017) 1026–1038, https://doi.org/10.1177/0885328216687665.

[231] T. Amna, M.S. Hassan, J. Yang, M.S. Khil, K.D. Song, J.D. Oh, I. Hwang, Virgin olive oil blended polyurethane micro/nanofibers ornamented with copper oxide nanocrystals for biomedical applications, Int. J. Nanomed. 9 (2014) 891–898, https://doi.org/10.2147/IJN.S54113.

[232] K. Yu, T. Zhu, Y. Wu, X. Zhou, X. Yang, J. Wang, J. Fang, H. El-Hamshary, S.S. Al-Deyab, X. Mo, Incorporation of amoxicillin-loaded organic montmorillonite into poly(ester-urethane) urea nanofibers as a functional tissue engineering scaffold,

Colloids Surfaces B Biointerfaces 151 (2017) 314–323, https://doi.org/10.1016/j.colsurfb.2016.12.034.

[233] I. Altinbasak, R. Jijie, A. Barras, B. Golba, R. Sanyal, J. Bouckaert, D. Drider, R. Bilyy, T. Dumych, S. Paryzhak, V. Vovk, R. Boukherroub, A. Sanyal, A. Sanyal, Sabine Szunerits, Reduced graphene-oxide-embedded polymeric nanofiber mats: an "on-demand" photothermally triggered antibiotic release platform, ACS Appl. Mater. Interfaces 10 (48) (2018) 41098–41106, https://doi.org/10.1021/acsami.8b14784.

[234] W. Jiang, M. Li, Z. Chen, K.W. Leong, Cell-laden microfluidic microgels for tissue regeneration, Lab Chip 16 (23) (2016) 4482–4506, https://doi.org/10.1039/c6lc01193d.

[235] D.B. Kolesky, R.L. Truby, A.S. Gladman, T.A. Busbee, K.A. Homan, J.A. Lewis, 3D bioprinting of vascularized, heterogeneous cell-laden tissue constructs, Adv. Mater. 26 (2014) 3124–3130, https://doi.org/10.1002/adma.201305506.

[236] S. Tasoglu, U. Demirci, Bioprinting for stem cell research, Trends Biotechnol. 31 (2013) 10–19, https://doi.org/10.1016/j.tibtech.2012.10.005.

[237] B. Guillotin, A. Souquet, S. Catros, M. Duocastella, B. Pippenger, S. Bellance, R. Bareille, M. Rémy, L. Bordenave, J. Amédée, F. Guillemot, Laser-assisted bio-printing of engineered tissue with high cell density and microscale organization, Biomaterials 31 (2010) 7250–7256, https://doi.org/10.1016/j.biomaterials.2010.05.055.

[238] V. Mironov, R.P. Visconti, V. Kasyanov, G. Forgacs, C.J. Drake, R.R. Markwald, Organ printing: tissue spheroids building blocks, Biomaterials 30 (2009) 2164–2174, https://doi.org/10.1016/j.biomaterials.2008.12.084.

[239] E.S. Bishop, S. Mostafa, M. Pakvasa, H.H. Luu, M.J. Lee, J.M. Wolf, G.A. Ameer, T.-C. He, R.R. Reid, 3-D bioprinting technologies in tissue engineering and re-generative medicine: current and future trends, Genes Dis 4 (4) (2017) 185–195, https://doi.org/10.1016/j.gendis.2017.10.002.

[240] F. Pati, J. Jang, D.-H. Ha, S.W. Kim, J.-W. Rhie, J.-H. Shim, D.-H. Kim, D.-W. Cho, Printing three-dimensional tissue analogues with decellularized extracellular matrix bioink, Nat. Commun. 5 (2014) 3935, https://doi.org/10.1038/ncomms4935.

[241] H.-W. Kang, S.J. Lee, I.K. Ko, C. Kengla, J.J. Yoo, A. Atala, A 3D bioprinting system to produce human-scale tissue constructs with structural integrity, Nat. Biotechnol. 34 (2016) 312–319, https://doi.org/10.1038/nbt.3413.

[242] Q. Gu, E. Tomaskoviccrook, R. Lozano, Y. Chen, R.M. Kapsa, Q. Zhou, G.G. Wallace, J.M. Crook, Functional 3D neural mini-tissues from printed gel-based bioink and human neural stem cells, Adv. Healthc. Mater. 5 (12) (2016) 1429–1438, https://doi.org/10.1002/adhm.201600095.

[243] F. Maiullari, M. Costantini, M. Milan, V. Pace, M. Chirivì, S. Maiullari, A. Rainer, D. Baci, H. El-S. Marei, D. Seliktar, C. Gargioli, C. Bearzi, R. Rizzi, A multi-cellular 3D bioprinting approach for vascularized heart tissue engineering based on HUVECs and iPSC-derived cardiomyocytes, Sci. Rep. 8 (2018) 13532, https://doi.org/10.1038/s41598-018-31848-x.

[244] T. Xu, J. Jin, C. Gregory, J.J. Hickman, T. Boland, Inkjet printing of viable mammalian cells, Biomaterials 26 (2005) 93–99, https://doi.org/10.1016/j.biomaterials.2004.04.011.

[245] R.E. Saunders, J.E. Gough, B. Derby, Delivery of human fibroblast cells by pie-zoelectric drop-on-demand inkjet printing, Biomaterials 29 (2008) 193–203, https://doi.org/10.1016/j.biomaterials.2007.09.032.

[246] X. Cui, T. Boland, Human microvasculature fabrication using thermal inkjet printing technology, Biomaterials 30 (31) (2009) 6221–6227, https://doi.org/10.1016/j.biomaterials.2009.07.056.

[247] R. Gaebel, N. Ma, J. Liu, J. Guan, L. Koch, C. Klopsch, M. Gruene, A. Toelk, W. Wang, P. Mark, F. Wang, B. Chichkov, W. Li, G. Steinhoff, Patterning human stem cells and endothelial cells with laser printing for cardiac regeneration, Biomaterials 32 (35) (2011) 9218–9230, https://doi.org/10.1016/j.biomaterials.2011.08.071.

[248] N.R. Schiele, D.T. Corr, Y. Huang, N.A. Raof, Y. Xie, D.B Chrisey, Laser-based direct-write techniques for cell printing, Biofabrication 2 (2010) 32001, https://doi.org/10.1088/1758-5082/2/3/032001.

[249] L. Koch, S. Kuhn, H. Sorg, M. Gruene, S. Schlie, R. Gaebel, B. Polchow, K. Reimers, S. Stoelting, N. Ma, P.M. Vogt, G. Steinhoff, B. Chichkov, Laser printing of skin cells and human stem cells, Tissue Eng. Part. C 16 (5) (2010) 847–854, https://doi.org/10.1089/ten.TEC.2009.0397.

[250] S. Ilkhanizadeh, A.I. Teixeira, O. Hermanson, Inkjet printing of macromolecules on hydrogels to steer neural stem cell differentiation, Biomaterials 28 (2007) 3936–3943, https://doi.org/10.1016/j.biomaterials.2007.05.018.

[251] E.D. Miller, K. Li, T. Kanade, L.E. Weiss, L.M. Walker, P.G. Campbell, Spatially directed guidance of stem cell population migration by immobilized patterns of growth factors, Biomaterials 32 (2011) 2775–2785, https://doi.org/10.1016/j.biomaterials.2010.12.005.

[252] A.D. Graham, S.N. Olof, M.J. Burke, J.P.K. Armstrong, E.A. Mikhailova, J.G. Nicholson, S.J. Box, F.G. Szele, A.W. Perriman, H. Bayley, High-resolution patterned cellular constructs by droplet-based 3D printing, Sci. Rep. 7 (2017) 7004, https://doi.org/10.1038/s41598-017-06358-x.

[253] Q. Chen, S. Utech, D. Chen, R. Prodanovic, J.M. Lin, D.A. Weitz, Controlled as-sembly of heterotypic cells in a core-shell scaffold: organ in a droplet, Lab Chip 16 (8) (2016) 1346–1349, https://doi.org/10.1039/C6LC00231E.

[254] H.F. Chan, Y. Zhang, K.W. Leong, Efficient one-step production of micro-encapsulated hepatocyte spheroids with enhanced functions, Small 12 (2016) 2720–2730, https://doi.org/10.1002/smll.201502932.

[255] D. Min, W. Lee, I.H. Bae, T.R. Lee, P. Croce, S.S. Yoo, Bioprinting of biomimetic skin containing melanocytes, Exp. Dermatol. 27 (5) (2018) 453–459, https://doi.org/10.1111/exd.13376.

[256] N. Mori, Y. Morimoto, S. Takeuchi, Skin integrated with perfusable vascular channels on a chip, Biomaterials 116 (2017) 48–56, https://doi.org/10.1016/j.biomaterials.2016.11.031.

[257] X.Q. Dou, C.L. Feng, Amino acids and peptide-based supramolecular hydrogels for three-dimensional cell culture, Adv. Mater. 29 (16) (2017) 1604062, https://doi.org/10.1002/adma.201604062.